Published in final edited form as:
Methods Enzymol. 2009 ; 454: 29–68. doi:10.1016/S0076-6879(08)03802-0.

Multiple Ion Binding Equilibria, Reaction Kinetics, and Thermodynamics in Dynamic Models of Biochemical Pathways

Kalyan C. Vinnakota[*], **Fan Wu**[*], **Martin J. Kushmerick**[†], and **Daniel A. Beard**[*]

[*] Biotechnology and Bioengineering Center and Department of Physiology, Medical College of Wisconsin, Milwaukee, Wisconsin

[†] Departments of Radiology, Bioengineering, Physiology and Biophysics, University of Washington, Seattle, Washington

Abstract

The operation of biochemical systems *in vivo* and *in vitro* is strongly influenced by complex interactions between biochemical reactants and ions such as H^+, Mg^{2+}, K^+, and Ca^{2+}. These are important second messengers in metabolic and signaling pathways that directly influence the kinetics and thermodynamics of biochemical systems. Herein we describe the biophysical theory and computational methods to account for multiple ion binding to biochemical reactants and demonstrate the crucial effects of ion binding on biochemical reaction kinetics and thermodynamics. In simulations of realistic systems, the concentrations of these ions change with time due to dynamic buffering and competitive binding. In turn, the effective thermodynamic properties vary as functions of cation concentrations and important environmental variables such as temperature and overall ionic strength. Physically realistic simulations of biochemical systems require incorporating all of these phenomena into a coherent mathematical description. Several applications to physiological systems are demonstrated based on this coherent simulation framework.

1. Introduction

1.1. The physicochemical basis of biology

It is essential that modern research in biology and biomedical science, which is increasingly focused on gaining quantitative understanding of the behavior of biochemical systems, be grounded in the physical chemical principles that govern the organization and behavior of matter. In particular, it is crucial to recognize that living systems, which continuously transport and transform material and transduce free energy among chemical, electrical, and mechanical forms, operate in nonequilibrium thermodynamic states. Thus effective characterization of the operation of living systems, through quantitative analysis and computational simulation, must account for the chemical thermodynamics of such systems. From this perspective, a useful characterization of a biological network includes an investigation and appreciation of its thermodynamic properties. Similarly, a realistic simulation of a biological system must be constrained to operate in a thermodynamically feasible manner.

1.2. Basic principles of chemical thermodynamics

The basic laws of thermodynamics are familiar to most readers. The two laws most relevant to systems biology may be stated as follow. (1) Energy is neither created nor destroyed; a net change in energy of a system must be due to a net transport of energy in or out. (2) In systems away from equilibrium, entropy is produced and never consumed; entropy may decrease only if the rate of export exceeds the rate of import.

By the second law, isolated systems move naturally in the direction of increasing entropy, always heading toward a thermodynamic equilibrium where the entropy is maximized. Yet biological systems are not isolated and, in the context of biology, equilibrium can be equated with death. Thus increasing entropy does not provide a gauge to predict or constrain the operation of biological systems that exchange material and energy with their environment. For such systems the concept of *free energy* provides a useful metric for describing thermodynamic status.

Various forms of free energy are defined for various sorts of systems. The most useful form of free energy for biological systems is Gibbs free energy, which is defined

$$G=E+PV-TS, \tag{2.1}$$

where E, P, V, T, and S, are the internal energy, pressure, volume, temperature, and entropy of the system. Gibbs free energy is a useful metric for biological systems because it can be shown that systems without import or export of chemical substances, held at constant pressure and temperature, spontaneously move down the gradient in G (Beard and Qian, 2008b).

For a chemical reaction in dilute solution the change in Gibbs free energy per number of times the reaction turns over is given by the well-known formula (Alberty, 2003; Beard and Qian, 2008b)

$$\Delta_r G=\Delta_r G^o+RT\sum_{i=1}^{N_s}\upsilon_i \ln\left(C_i/C_o\right), \tag{2.2}$$

where $\Delta_r G^o$ is the equilibrium free energy for the reaction, which does not depend on the concentrations of the chemical components, R is the gas constant, T is the absolute temperature, υ_i is the stoichiometric number of species i for the reaction, C_i is the concentration of species I, and C_o is the reference concentration, taken to be 1 M. The summation in Eq. (2.2) is over all species in the system; N_s is the number of species.

The equilibrium free energy for a reaction may be computed based on the values of free energy of formation, $\Delta_f G_i^o$, for the species involved in a reaction:

$$\Delta_r G^o=\sum_{i=1}^{N_s}\Delta_f G_i^o. \tag{2.3}$$

The value of $\Delta_f G_i^o$ for a given species depends on the environmental conditions, most notably temperature, pressure, and the ionic solution strength, as discussed later. Chemical equilibrium is achieved when the driving force for the reaction $\Delta_r G$ goes to zero. Equilibrium yields

$$\begin{aligned} -\frac{\Delta_r G^o}{RT}&=\sum_{i=1}^{N_s}\upsilon_i \ln\left(C_i/C_o\right)=\ln\prod_{i=1}^{N_s}\left(C_i/C_o\right)^{\upsilon_i}\\ \exp\left(-\frac{\Delta_r G^o}{RT}\right)&=K_{eq}=\prod_{i=1}^{N_s}\left(C_i/C_o\right)^{\upsilon_i}, \end{aligned} \tag{2.4}$$

where K_{eq} is the equilibrium constant for the reaction.

1.3. Simulating biochemical systems

In living systems operating away from equilibrium, each chemical process (including reactions and transport processes) obeys the following relationship between flux and free energy:

$$J^+/J^- = e^{-\Delta G/RT}, \tag{2.5}$$

where $J = J^+ - J^-$ is the net flux for the process and J^+ and J^- are the forward and reverse fluxes. For example, for an enzyme-catalyzed reaction, J^+ and J^- are the forward and reverse rates of turnover for the enzyme's catalytic cycle.

Equation (2.5) reveals that nonzero net flux occurs only when the free energy change for a given process is nonzero. Also, it is apparent that the quantity

$$-\Delta G \cdot J = RT \ln (J^+/J^-) \cdot (J^+ - J^-) \tag{2.6}$$

is always positive. In fact, $-\Delta G \cdot J$ is the process's rate of free energy dissipation. Thus it follows that systems maintained away from equilibrium dissipate free energy. Dissipation of free energy is a hallmark of nonequilibrium systems and thus a hallmark of life.

At the center of our biochemical systems modeling approach is an explicit accounting of the fact that biochemical reactants (e.g., ATP) exist in solution as a number of rapidly interconverting species (e.g., ATP^{4-}, $HATP^{3-}$, $MgATP^{2-}$, and $KATP^{3-}$)(Beard and Qian, 2008a, c). Accounting for all of these species for systems composed of many (tens to hundreds) of reactants is theoretically straightforward, but practically messy. Notably, Wu and colleagues (2007b) have detailed how a model of nontrivial complexity is constructed. However, before going into computational details, the following list is a number of benefits of accounting for this level of chemical detail in biochemical systems simulation.

1. Nonambiguous meaning. By tracking the species-level distribution of biochemical reactants, model variables have a nonambiguous physical meaning. Because species participate in enzyme-catalyzed reactions, a species-level model allows us to represent chemical reactions with greater physical realism than is possible when the species distributions of reactants are not calculated. By expressing enzyme mechanisms in terms of species, changes in apparent kinetic properties brought on by changes in pH and ion concentration are handled explicitly. More details on this point are provided in Section 2.5 and in Beard *et al*. (2008).
2. Nonambiguous integration. In biosystems modeling it is common to track certain species but not others. For example, some models of cellular energetics account for Mg^{2+}-bound and -unbound ATP (Korzeniewski, 2001; Vendelin *et al*., 2000, 2004). However, in these cases the unbound state is a mixture of many states. Other modeling applications may be based on treating all reactants, including ATP, as the total sum of species (Zhou *et al*., 2005). As a result, there is often not one unique way to integrate models that simulate different components of a larger system. By imposing a formalism where model variables have nonambiguous meaning this problem of nonuniqueness is resolved.
3. Resulting models are thermodynamically feasible. By computing species distribution of reactants, we can track how changes in pH and cationic concentrations affect overall thermodynamic driving forces and ensure that these changes are handled by our

models. Thus simulation at this level of detail ensures thermodynamically validity, an important requirement for model reliability.

4. Model uncertainty is reduced. One might imagine that imposing the level of detail outlined previously may introduce unnecessary complexity and increase the number of unknown parameters into biochemical systems models. However, the opposite is true when ionic dissociation constants and basic thermodynamic data are available for the reactions and reactants in a given model. The thermodynamic and dissociation data constrain the enzyme mechanisms and reduce the number of adjustable parameters necessary to describe their behavior.

   In addition to these practical advantages related to model building and identification, the major advantage is scientific.

5. Model reliability is improved. We have greater confidence in the behavior predicted by physically grounded models than in models that invoke phenomenological descriptions of components or in models that do not account for chemical species distribution and/or biochemical thermodynamics. This is particularly important when using models to predict behavior outside of the operational regime of the data set(s) used for parameterization and validation.

2. Biochemical Conventions and Calculations

Equation (2.2) is the formula for Gibbs free energy for a chemical reaction. However, biochemical reactions are not typically expressed as mass-and charge-balanced chemical reactions Alberty (2003).

2.1. Thermodynamics of biochemical reactions

Metabolites in intracellular milieu exist as protonated, metal ion bound and free unbound forms described by ionic equilibria in solution with multiple cations. Each metabolite concentration is therefore described as a sum of its individual constituent species concentrations computed by ionic equilibria principles. A biochemical reaction involves sums of species on both the reactant and the product sides, which results in each reaction having effective proton and metal ion stoichiometries due to binding changes across the biochemical reaction. The proton generation stoichiometry of a biochemical reaction is the total difference of average proton binding between the reactants and the products, plus the proton generation stoichiometry of the reaction defined in terms of its most unbound species in the pH range of interest, also known as the reference reaction. The apparent equilibrium constant of a biochemical reaction defined in terms of sums of species for each metabolite therefore depends on proton and metal binding of the reactants and products.

Alberty developed these concepts in terms of transformed variables by using Legendre transforms to gain a global view of biochemical systems by treating pH and free magnesium ion concentrations as independent variables. Fundamental principles underlying this work are reviewed in Alberty (2004). More detailed treatment of this subject matter and basic biochemical data and calculations are given in Alberty (2003). Vinnakota *et al*. (2006) extended the application of concepts developed by Alberty to a system with finite buffer capacity and variable pH. The pH variation itself is computed from proton binding changes in each of the biochemical reactions. Using mass balance constraint for protons and Mg^{2+} ions, we applied these concepts to compute a pH time course while accounting for pH, Mg^{2+}, and K^{+} effects on kinetics and thermodynamics of the reactions. The methodology in Vinnakota *et al*. (2006) was extended and improved by Wu *et al*. (2007b) and Beard and Qian (2008a) to account for more metal ions and was applied to coupled electrophysiological and metabolic systems.

During the past decade, tables of fundamental biochemical data have been generated by Alberty (2003), which enabled the computation of standard free energies of many biochemical reactions in terms of their reference species and therefore their apparent equilibrium constants at specified pH and metal ion concentrations. The methods presented here demonstrate that the thermodynamic analysis and the biochemical network representation are unified through proton and other metal ion mass balance constraints.

2.2. Enzyme kinetics and the Haldane constraint

Thermodynamic analyses predict equilibria for pathways at specified pH, temperature, ionic strength, ion concentrations, and cofactor concentrations. However, this gives only part of the picture, because the kinetics govern the dynamics of approach of biochemical systems to these equilibria in a closed system and in an open system the combined effect of kinetics constrained by thermodynamics govern the fluxes and the metabolite transients. Likewise, kinetic models with inappropriate thermodynamic constraints will not yield a realistic prediction of fluxes and concentrations, as the apparent equilibrium constant can change by orders of magnitude per unit pH depending on the proton stoichiometry of the biochemical reaction. These two approaches can be combined by incorporating the apparent equilibrium constant computed by biochemical thermodynamic principles into the Haldane relationship, which relates the forward and reverse maximal velocities of the enzyme kinetic flux. This unified approach combining both kinetics and thermodynamics is applied in Vinnakota *et al*. (2006), Wu *et al*. (2007b, 2008), and Beard and Qian (2008a). Alberty (2006) has demonstrated that the overall apparent equilibrium constant of a biochemical reaction is independent of the internal enzyme kinetic mechanisms for simple enzyme kinetic mechanisms.

While the study of the catalytic kinetics of enzymes represents one of the most established and well-documented fields in biochemical research, the impact of the biochemical state (pH, ionic strength, temperature, and certain cation concentrations) is typically not formally accounted for in kinetic studies (Alberty, 1993, 2006). *In vitro* experiments using purified proteins and controlled substrate concentrations to characterize enzyme kinetics are conducted under conditions that do not necessarily match the physiological environment, but are determined based on a number of factors, including the requirements of the assays used to measure the kinetics. Therefore, it is difficult to compare results obtained from different studies and to use available kinetic data to predict *in vivo* function without ambiguity.

Outlining these and other issues in somewhat greater detail, the following specific challenges associated with interpreting *in vitro* kinetic data must be overcome to make optimal use of them.

1. While a great deal of high-quality data may be available for a particular enzyme, much of these data were obtained in the 1960s and 1970s when tools for proper analysis of data were not available. As a result, the reported kinetic parameter values [typically obtained from double reciprocal plots of inverse flux versus inverse substrate (Lineweaver and Burk, 1934)] may not optimally match reported data.
2. Data on biochemical kinetics are typically obtained under nonphysiological pH and ionic conditions. Therefore the reported kinetic constants must be corrected to apply to simulations of physiological systems.
3. A third problem related to the second is that kinetic constants are associated with apparent mechanisms that operate on biochemical reactants, which are sums of biochemical species (Alberty, 1993). The result is that the reported mechanisms and associated parameter values are dependent on the biochemical state and not easily translated to apply to different biochemical states or to simulations in which the biochemical state changes.

4. The reported kinetic mechanisms and parameters are often not constrained to match thermodynamic data for a given reaction. Since the basic thermodynamics of a given reaction is typically characterized with greater precision than the kinetics of an enzyme catalyzing the reaction, putative kinetic mechanisms should be constrained to match the biochemical reaction thermodynamics.

A study on citrate synthase addressed and corrected these problems by posing reaction mechanisms in terms of species and ensuring that mechanisms properly account for thermodynamics. This basic approach was first introduced by Frieden and Alberty (1955), yet has received little attention. By reanalyzing legacy data from a variety of sources of kinetic data on citrate synthase, for example, we are able to show that data used to support the consensus model of the mechanism for this enzyme (random bi-bi mechanism) are all consistent with the compulsory-order ternary-complex mechanism and not consistent with the random bi-bi model (Beard *et al*., 2008).

2.3. Multiple cation equilibria in solutions: Apparent equilibrium constant, buffering of cations, and computing time courses of cations as a consequence of biochemical reaction networks

Most metabolites in physiological milieu are anionic and bind to H^+, Mg^{2+}, K^+, and Ca^{2+} ions in rapid equilibrium. To compute the distribution of a metabolite into ion bound and unbound species, we choose as a reference form the species with no dissociable protons or metal ions in the pH range of 5–9 for physiological models. Based on this definition, the following steps and calculations are needed to account for H^+ and metal cation binding to metabolites, buffer capacity and pH change, and the effects of these parameters on reaction equilibria.

1. Based on binding equilibria, the total concentration of a biochemical reactant is defined in terms of its reference species concentration and the free concentrations of ions and their binding affinities.
2. On the basis of the definition of reference and biochemical reactions, the reference and apparent equilibrium constants of each biochemical reaction are computed. The apparent equilibrium constant is a function of the reference equilibrium constant and the binding polynomials of the reactants and the products. The apparent equilibrium constant constrains the enzyme kinetic flux through the Haldane relationship.
3. The flux through each biochemical reaction is derived on the basis of a detailed catalytic scheme. The reference reaction is balanced with respect to mass and charge and has a reference proton stoichiometry.
4. The coupled differential equations for ion and biochemical reactant concentrations are integrated to simulate the system dynamics.

2.3.1. Calculation of proton binding fraction for each metabolite using multiple cation equilibria—A biochemical reactant in physiological milieu exists in different ion bound species in rapid equilibrium. These ions include H^+, Mg^{2+}, K^+, and other cations. Multiple cation equilibria principles are used to describe the distribution of each biochemical reactant in various ion bound species. For example, the reactant phosphocreatine (PCr) will exist in the following forms:

$$[\mathrm{PCr}_{total}]=[\mathrm{HPCr}^{2-}]+[\mathrm{H_2PCr}^{-}]+[\mathrm{MgHPCr}]+[\mathrm{KHPCr}^{-}]. \quad (2.7)$$

Each ion bound species is in turn computed in terms of an equilibrium relationship between the most unbound form of the reactant and the metal ion that it binds to. Detailed examples are

provided in Sections 2.4 and 2.5. Table 2.1 defines the conventions and nomenclature used in our biochemical models.

In general, let [L] represent the concentration of unbound anionic form of biochemical reactant L and [L_{total}] be its total concentration in all forms. The total concentration is expressed as

$$[L_{total}]=[L]+\sum_{p=1}^{N_p}[LH_p]+\sum_{m=1}^{N_m}[LM^m], \tag{2.8}$$

where [LH_p] is L bound to p [H^+] ions and N_p is the highest number of protons that can bind to L; [LM^m] is L bound to the mth metal ion. The second term on the right refers to the sum of the proton bound forms, and the third term refers to the sum of the metal bound forms. Any number of cations can be included in this scheme if their dissociation constants are known for a given reactant. For simplicity, we assume that at most only one metal ion of each type binds to L. Note that the net charge on each of the species is not stated here for simplicity of notation, but this quantity is equal to the sum of the charge of the reference species and the total charge of the metal ions bound for each species. The concentration [LH_p] is given by the equilibrium relation:

$$[LH_p]=\frac{[L]\,[H^+]^p}{\prod_{l=1}^{p}K_{a,l}},\ p\geq 1, \tag{2.9}$$

where $K_{a,l}$ is the dissociation constant for the reaction, [LH_l] $\rightleftharpoons$ [LH_{l-1}] + [H^+] and $K_{a,l}=\left(\frac{[H^+]\,[LH_{l-1}]}{[LH_l]}\right)_{eq}$ at a given temperature and ionic strength.

For example, for phosphocreatine, $[H_2PCr^-]=\frac{[HPCr^{2-}]\,[H^+]}{K_{a,1}}$.

The dissociation constants [usually expressed as $pKa = -\log_{10}(K_a)$] are obtained from sources such as the NIST Database 46. Typically, these pK values must be recalculated for specific temperature and ionic strength to be simulated. The following equation can be applied for the temperature correction (Alberty, 2003):

$$pKa_{T_2}=pKa_{T_1}+\left(\frac{1}{T_2}-\frac{1}{T_1}\right)\cdot\frac{\Delta H^0}{2.303\cdot R}, \tag{2.10}$$

where T_1 is the temperature at which the pK was reported in the database, T_2 is the temperature at which pKa_{T2} is calculated, and R =8.314 JK^{-1} mol^{-1} is the universal gas constant.

The enthalpy of dissociation reactions is a function of ionic strength. The following empirical equation (Alberty, 2003) gives ionic strength dependence of enthalpy at 298.15 K:

$$\Delta H^0=\Delta H^0(I=0)+\frac{1.4775I^{1/2}\sum\nu_i z_i^2}{1+1.6I^{1/2}}. \tag{2.11}$$

The effects of ionic strength on *pK* can be approximated using the following empirical equation (Alberty, 2003):

$$pKa(I)=pKa(I_1)+\frac{1.17582}{2.303}\left(\frac{I_1^{1/2}}{1+1.6I_1^{1/2}}-\frac{I^{1/2}}{1+1.6I^{1/2}}\right)\sum \nu_i z_i^2. \tag{2.12}$$

The numerical constants in Eqs. (2.11) and (2.12) are derived from Alberty's fits to experimental data from Clarke and Glew (1980) as described in Alberty (2003). In summary, the *pK* at a given temperature and ionic strength is corrected for the desired ionic strength using Eq. (2.12). A temperature-corrected value is then obtained from Eq. (2.10) in which the dissociation enthalpy is first corrected for ionic strength using Eq. (2.11).

The concentration of each of the *m*th metal bound species $[LM^m]$ is given by

$$[LM^m]=\frac{[L]\,[M^m]}{K_{M,m}}, \tag{2.13}$$

where $K_{M,m}$ is the dissociation constant for metal ion $[M^m]$ binding to [L]. We assume in Eq. (2.13) that each species binds at most one metal ion per molecule.

The concentration of bound protons due to each bound form $[LH_p]$ with *p* dissociable protons is given by $p[LH_p]$. The sum total of bound proton concentration is given by $\sum_{p=1}^{N_p} p[LH_p]$ for the biochemical reactant *L*.

For example, for phosphocreatine, $[MgHPCr]=\frac{[HPCr^{2-}][Mg^{2+}]}{K_{Mg}}$.

The average proton binding for biochemical reactant L is the ratio of bound proton concentration to total concentration of L, which is given by

$$\overline{N}_H^L=\frac{\sum_{p=1}^{N_p} p[LH_p]}{[L_{total}]}=\frac{\sum_{p=1}^{N_p} p[LH_p]}{[L]+\sum_{p=1}^{N_p}[LH_p]+\sum_{m=1}^{N_m}[LM^m]}$$
$$=\frac{\sum_{p=1}^{N_p}\frac{p[L]\,[H]^p}{p\prod_{l=1}K_{a,l}}}{[L]+\sum_{p=1}^{N_p}\frac{[L]\,[H^+]^p}{p\prod_{l=1}K_{a,l}}+\sum_{m=1}^{N_m}\frac{[L]\,[M^m]}{K_{M,m}}}=\frac{\sum_{p=1}^{N_p}\frac{p[H^+]^p}{p\prod_{l=1}K_{a,l}}}{P_L} \tag{2.14}$$

where P_L is defined as the binding polynomial of *L*.

$$P_L = 1 + \sum_{p=1}^{N_p} \frac{[\mathrm{H}^+]^p}{\prod_{l=1}^{p} K_{a,l}} + \sum_{m=1}^{N_m} \frac{[\mathrm{M}^m]}{K_{M,m}} \tag{2.15}$$

For example, the binding polynomial for phosphocreatine would be written as

$$P_L = 1 + \frac{[\mathrm{HPCr}^{2-}][\mathrm{H}^+]}{K_{a,1}} + \frac{[\mathrm{HPCr}^{2-}][\mathrm{Mg}^{2+}]}{K_{Mg}} + \frac{[\mathrm{HPCr}^{2-}][\mathrm{K}^+]}{K_K}. \tag{2.16}$$

A similar expression can be written for average metal ion binding, where the numerator contains metal ion binding equilibria instead of just proton binding equilibria. The number p in Eqs. (2.8) and (2.14) denotes the number of dissociable protons bound in each proton bound form of the metabolite L. Note that the product of [L] and P_L gives [L_{total}] and that each term the binding polynomial represents the ratio of the unbound, proton bound, and metal ion bound forms of L to the unbound form of L.

2.3.2. Reference and biochemical reactions and the flux through an enzyme catalyzed reaction—We define the reference species of the biochemical reactant as the most deprotonated species in the pH range 5.5–8.5, which are used to calculate the average proton binding $\overline{N}_H^L$ for each biochemical reactant L. As an example the creatine kinase reaction is shown here in terms of its reference species to illustrate this point:

$$\mathrm{HPCr}^{2-} + \mathrm{ADP}^{3-} + \mathrm{H}^+ \rightleftarrows \mathrm{HCr}^0 + \mathrm{ATP}^{4-}. \tag{2.17}$$

The biochemical reaction associated with this reference reaction is defined in terms of sums of species constituting each of the reactants and products:

$$\mathrm{PCr}_{\mathrm{total}} + \mathrm{ADP}_{\mathrm{total}} \rightleftarrows \mathrm{Cr}_{\mathrm{total}} + \mathrm{ATP}_{\mathrm{total}}. \tag{2.18}$$

The average proton generation stoichiometry, $\Delta_r N_H$ of the biochemical reaction, is the difference between the average proton binding of the reactants and the products plus the proton generation stoichiometry, n, of the reference reaction:

$$\Delta_r N_H = \sum_{\mathrm{reactants}} \overline{N}_H^{\mathrm{reactant}} - \sum_{\mathrm{products}} \overline{N}_H^{\mathrm{product}} + n. \tag{2.19}$$

Defined in this way, n is an integer but $\Delta_r N_H$ is not because the first two terms on the right-hand side of Eq. (2.19), which are sums of average proton binding of the reactants and the products computed from Eq. (2.14), are nonintegers. Note that the first two terms on the right-hand side of Eq. (2.19) go to zero at highly alkaline pH values. For a system of reactions we define $\Delta_r N_H^k$ and n_k as the proton generation stoichiometries of the biochemical and reference reactions, respectively, for the kth reaction.

The proton generation flux through a reaction is given by the product of the proton stoichiometry for that reaction and the flux through the reaction. For a set of reactions in a

system, the total proton generation flux is given by a summation of the individual proton fluxes for all biochemical reactions:

$$\text{Proton flux} = \sum_{k=1}^{N_r} \Delta_r N_H^k J_k, \tag{2.20}$$

where J_k is the flux through the kth biochemical reaction.

2.3.3. Apparent equilibrium constant and the Haldane constraint—Changes in the apparent equilibrium constant due to pH and other cations will impact the reverse V_{max} as defined in the model by the Haldane relationship. The standard free energy of the kth reference reaction is the difference between the free energies of formation of the products and the reactants in that reaction:

$$\Delta_r G_k^0 = \sum_j \nu_j^k \Delta_f G_j^0. \tag{2.21}$$

The free energy of formation of each reference species is a function of ionic strength:

$$\Delta_f G_j^0 = \Delta_f G_j^0(I=0) - \frac{2.91482 z_j^2 I^{1/2}}{1+1.6 I^{1/2}}. \tag{2.22}$$

Since the reference reaction is balanced with respect to protons, the free energy of the reference reaction, $\Delta_r G_k^0$, is independent of pH and therefore a constant at a given ionic strength and temperature.

The equilibrium constant of the reference reaction is given by

$$K_{ref}^k = e^{-\Delta_r G_k^0 / RT}. \tag{2.23}$$

The apparent equilibrium constant of a biochemical reaction is defined in terms of the metabolite concentrations at equilibrium [indicated by the subscript "*eq*" in Eq. (24)], which are sums of their constituent species:

$$K_{app}^k = \frac{\prod [L_{total}^{\text{product}} / c_0]_{eq}^{\nu^k_{\text{product}}}}{\prod [L_{total}^{\text{reactant}} / c_0]_{eq}^{\nu^k_{\text{reactant}}}} = K_{ref}^k [\text{H}^+]^{-n_k} \frac{\prod P_{products}}{\prod P_{reactants}}, \tag{2.24}$$

where n_k is the proton stoichiometry of the reference reaction and P is the binding polynomial for a biochemical reactant as defined in Eq. (2.15).

The standard free energy for a biochemical reaction is given by

$$\Delta_r G'^0_k = -RT \ln (K_{app}^k). \tag{2.25}$$

2.3.4. Ion mass balance and the differential equations for ion concentrations—

The differential equation for a particular ion concentration is derived from a statement of mass conservation for that ion. For metal ions, the total concentration (bound plus free) concentration is

$$[\mathrm{M}^{z_j+}_{j,total}]=[\mathrm{M}^{z_j+}_{j}]+[\mathrm{M}^{z_j+}_{j,bound}], \tag{2.26}$$

where $[\mathrm{M}^{z_j+}_{j}]$ is the *j*th free metal ion concentration and $[\mathrm{M}^{z_j+}_{j,total}]$ is the metabolite bound dissociable metal ion concentration.

The conservation equation for protons includes an additional term for covalently bound protons in reference species:

$$[\mathrm{H}^{+}_{total}]=[\mathrm{H}^{+}]+[\mathrm{H}^{+}_{bound}]+[\mathrm{H}^{+}_{reference}], \tag{2.27}$$

where $[\mathrm{H}^{+}_{reference}]$ denotes the protons in reference species.

In a closed system, the total proton pool is constant ($\frac{d[\mathrm{H}^{+}_{total}]}{dt}=0$). Differentiating Eq. (2.27) for proton conservation with respect to time, we get

$$0=\frac{d[\mathrm{H}^{+}]}{dt}+\frac{d[\mathrm{H}^{+}_{bound}]}{dt}+\frac{d[\mathrm{H}^{+}_{reference}]}{dt}. \tag{2.28}$$

The second term in Eq. (2.28) can be expanded by using the chain rule:

$$\frac{d[\mathrm{H}^{+}_{bound}]}{dt}=\frac{\partial[\mathrm{H}^{+}_{bound}]}{\partial[\mathrm{H}^{+}]}\frac{d[\mathrm{H}^{+}]}{dt}+\sum_j\frac{\partial[\mathrm{H}^{+}_{bound}]}{\partial[\mathrm{M}^{z_j+}_{j}]}\frac{d[\mathrm{M}^{z_j+}_{j}]}{dt}+\sum_i\frac{\partial[\mathrm{H}^{+}_{bound}]}{\partial[\mathrm{L}_i]}\frac{d[\mathrm{L}_i]}{dt}. \tag{2.29}$$

The third term is obtained from summation of the product of proton stoichiometry of each of the reference reactions with the flux through the reaction (generation of free protons from the reference pool diminishes the reference pool):

$$\frac{d[\mathrm{H}^{+}_{reference}]}{dt}=-\sum_{k=1}^{N_r}n_kJ_k. \tag{2.30}$$

Using Eqs. (2.29) and (2.30) in Eq. (2.28) and transposing terms, we obtain the following equation for $d[\mathrm{H}^{+}]/dt$:

$$\frac{d[\mathrm{H}^{+}]}{dt}=\frac{-\sum_j\frac{\partial[\mathrm{H}^{+}_{bound}]}{\partial[\mathrm{M}^{z_j+}_{j}]}\frac{d[\mathrm{M}^{z_j+}_{j}]}{dt}-\sum_i\frac{\partial[\mathrm{H}^{+}_{bound}]}{\partial[\mathrm{L}_i]}\frac{d[\mathrm{L}_i]}{dt}+\sum_{k=1}^{N_r}n_kJ_k}{1+\frac{\partial[\mathrm{H}^{+}_{bound}]}{\partial[\mathrm{H}^{+}]}}. \tag{2.31}$$

When hydrogen ion is transported into and out of the system, this equation becomes

$$\frac{d[\mathrm{H}^+]}{dt}=\frac{-\sum_j \frac{\partial[\mathrm{H}^+_{bound}]}{\partial[\mathrm{M}_j^{z_j+}]}\frac{d[\mathrm{M}_j^{z_j+}]}{dt}-\sum_i \frac{\partial[\mathrm{H}^+_{bound}]}{\partial[\mathrm{L}_i]}\frac{d[\mathrm{L}_i]}{dt}+\sum_{k=1}^{N_r} n_k J_k + J_t^{\mathrm{H}}}{1+\frac{\partial[\mathrm{H}^+_{bound}]}{\partial[\mathrm{H}^+]}}, \tag{2.32}$$

where J_t^{H} is the flux of [H^+] transport into the system.

Similarly, the rate of change of each metal ion [$\mathrm{M}_j^{z_j+}$] is written as

$$\frac{d[\mathrm{M}_j^{z_j+}]}{dt}=\frac{-\frac{\partial[\mathrm{M}_{j,bound}^{z_j+}]}{\partial[\mathrm{H}^+]}\frac{d[\mathrm{H}^+]}{dt}-\sum_l \frac{\partial[\mathrm{M}_{j,bound}^{z_j+}]}{\partial[\mathrm{M}_l^{z_l+}]}\frac{d[\mathrm{M}_l^{z_l+}]}{dt}-\sum_i \frac{\partial[\mathrm{M}_{j,bound}^{z_j+}]}{\partial[\mathrm{L}_i]}\frac{d[\mathrm{L}_i]}{dt}+J_t^{\mathrm{M}_j}}{1+\frac{\partial[\mathrm{M}_{j,bound}^{z_j+}]}{\partial[\mathrm{M}_j^{z_j+}]}}. \tag{2.33}$$

For a total of N_j metal ions, Eq. (2.33) plus either Eq. (2.31) or Eq. (2.32) results in N_j + 1 coupled differential equations for the ion concentrations. Solving for the time derivatives, we can obtain N_j + 1 differential equations for the ion concentration time derivatives that may be numerically integrated simultaneously with the N_L differential equations for the biochemical reactants [$L_{total,\,i}$].

The set of differential equations for biochemical reactant L_i is given by

$$\frac{d[\mathrm{L}_{total,i}]}{dt}=\sum_k \nu_k^i J_k, \tag{2.34}$$

where ν_k^i is the stoichiometry of the *i*th metabolite in the *k*th reaction and J_k is the flux through the *k*th reaction.

As an example, we apply these general equations to treat muscle cell cytoplasm. The cation species in cardiac and skeletal muscle cell cytoplasm that significantly influence the kinetics and apparent equilibrium constants of biochemical reactions are H^+, Mg^{2+}, and K^+. The Ca^{2+} ion is also an important second messenger for cellular processes whose concentration changes by at least two orders of magnitude during rest and mechanical contraction (Guyton and Hall, 2006). However, the contribution of Ca^{2+} to the binding polynomial of most metabolites is much smaller when compared to that of H^+, Mg^{2+}, and K^+. For each reactant in the cytoplasm, the binding polynomial is

$$P_i([\mathrm{H}^+],[\mathrm{M}g^{2+}],[\mathrm{K}^+])=1+[\mathrm{H}^+]/K_i^{\mathrm{H}}+[\mathrm{Mg}^{2+}]/K_i^{Mg}+[\mathrm{K}^+]/K_i^{K}, \tag{2.35}$$

where K_i^H, K_i^{Mg}, and K_i^K are the binding constants for H^+, Mg^{2+}, and K^+. Here we consider only one binding reaction per ion per reactant. Following Eqs. (2.32) and (2.33), we can write the differential equations for the H^+, Mg^{2+}, and K^+ concentrations:

$$\frac{d[\mathrm{H}^+]}{dt}=\frac{-\frac{\partial[\mathrm{H}_{bound}]}{\partial[\mathrm{Mg}^{2+}]}\frac{d[\mathrm{Mg}^{2+}]}{dt}-\frac{\partial[\mathrm{H}_{bound}]}{\partial[\mathrm{K}^+]}\frac{d[\mathrm{K}^+]}{dt}-\frac{\partial[\mathrm{H}_{bound}]}{\partial[\mathrm{L}_i]}\frac{d[\mathrm{L}_i]}{dt}+\sum_{k=1}^{N_f}n_kJ_k+J_t^{\mathrm{H}}}{1+\frac{\partial[\mathrm{H}_{bound}]}{\partial[\mathrm{H}^+]}} \tag{2.36}$$

$$\frac{d[\mathrm{Mg}^{2+}]}{dt}=\frac{-\frac{\partial[\mathrm{Mg}_{bound}]}{\partial[\mathrm{H}^+]}\frac{d[\mathrm{H}^+]}{dt}-\frac{\partial[\mathrm{Mg}_{bound}]}{\partial[\mathrm{K}^+]}\frac{d[\mathrm{K}^+]}{dt}-\frac{\partial[\mathrm{Mg}_{bound}]}{\partial[\mathrm{L}_i]}\frac{d[\mathrm{L}_i]}{dt}+J_t^{Mg}}{1+\frac{\partial[\mathrm{Mg}_{bound}]}{\partial[\mathrm{Mg}^{2+}]}} \tag{2.37}$$

$$\frac{d[\mathrm{K}^+]}{dt}=\frac{-\frac{\partial[\mathrm{K}_{bound}]}{\partial[\mathrm{H}^+]}\frac{d[\mathrm{H}^+]}{dt}-\frac{\partial[\mathrm{K}_{bound}]}{\partial[\mathrm{Mg}^{2+}]}\frac{d[\mathrm{Mg}^{2+}]}{dt}-\frac{\partial[\mathrm{K}_{bound}]}{\partial[\mathrm{L}_i]}\frac{d[\mathrm{L}_i]}{dt}+J_t^{K}}{1+\frac{\partial[\mathrm{K}_{bound}]}{\partial[\mathrm{K}^+]}}. \tag{2.38}$$

These equations can be solved as a system of linear equations for the derivatives of $[H^+]$, $[Mg^{2+}]$, and $[K^+]$. We now define the expressions for partial derivatives and buffering terms based on the binding polynomial defined in Eq. (2.35):

$$\frac{\partial[\mathrm{H}_{bound}]}{\partial[\mathrm{Mg}^{2+}]}=-\sum_{i=1}^{N_r}\frac{[\mathrm{L}_i][\mathrm{H}^+]/K_i^{\mathrm{H}}}{K_i^{Mg}\left(P_i([\mathrm{H}^+],[\mathrm{Mg}^{2+}],[\mathrm{K}^+])\right)^2}, \tag{2.39}$$

$$\frac{\partial[\mathrm{H}_{bound}]}{\partial[\mathrm{K}^+]}=-\sum_{i=1}^{N_r}\frac{[\mathrm{L}_i][\mathrm{H}^+]/K_i^{\mathrm{H}}}{K_i^{K}\left(P_i([\mathrm{H}^+],[\mathrm{Mg}^{2+}],[\mathrm{K}^+])\right)^2}, \tag{2.40}$$

$$\frac{\partial[\mathrm{H}_{bound}]}{\partial[\mathrm{H}^+]}=\sum_{i=1}^{N_r}\frac{[\mathrm{L}_i](1+[\mathrm{Mg}^{2+}]/K_i^{Mg}+[\mathrm{K}^+]/K_i^{K})}{K_i^{\mathrm{H}}\left(P_i([\mathrm{H}^+],[\mathrm{Mg}^{2+}],[\mathrm{K}^+])\right)^2}, \tag{2.41}$$

$$\frac{\partial[\mathrm{Mg}_{bound}]}{\partial[\mathrm{H}^+]}=-\sum_{i=1}^{N_r}\frac{[\mathrm{L}_i][\mathrm{Mg}^{2+}]/K_i^{Mg}}{K_i^{\mathrm{H}}\left(P_i([\mathrm{H}^+],[\mathrm{Mg}^{2+}],[\mathrm{K}^+])\right)^2}, \tag{2.42}$$

$$\frac{\partial[\mathrm{Mg}_{bound}]}{\partial[\mathrm{K}^+]}=-\sum_{i=1}^{N_r}\frac{[\mathrm{L}_i][\mathrm{Mg}^{2+}]/K_i^{Mg}}{K_i^{K}\left(P_i([\mathrm{H}^+],[\mathrm{Mg}^{2+}],[\mathrm{K}^+])\right)^2}, \tag{2.43}$$

$$\frac{\partial[\mathrm{Mg}_{bound}]}{\partial[\mathrm{Mg}^{2+}]}=\sum_{i=1}^{N_r}\frac{[\mathrm{L}_i](1+[\mathrm{H}^+]/K_i^{\mathrm{H}}+[\mathrm{K}^+]/K_i^K)}{K_i^{Mg}\left(P_i([\mathrm{H}^+],[\mathrm{Mg}^{2+}],[\mathrm{K}^+])\right)^2}, \tag{2.44}$$

$$\frac{\partial[\mathrm{K}_{bound}]}{\partial[\mathrm{H}^+]}=-\sum_{i=1}^{N_r}\frac{[\mathrm{L}_i][\mathrm{K}^+]/K_i^K}{K_i^{\mathrm{H}}\left(P_i([\mathrm{H}^+],[\mathrm{Mg}^{2+}],[\mathrm{K}^+])\right)^2}, \tag{2.45}$$

$$\frac{\partial[\mathrm{K}_{bound}]}{\partial[\mathrm{Mg}^{2+}]}=-\sum_{i=1}^{N_r}\frac{[\mathrm{L}_i][\mathrm{K}^+]/K_i^K}{K_i^{Mg}\left(P_i([\mathrm{H}^+],[\mathrm{Mg}^{2+}],[\mathrm{K}^+])\right)^2}, \tag{2.46}$$

$$\frac{\partial[\mathrm{K}_{bound}]}{\partial[\mathrm{K}^+]}=\sum_{i=1}^{N_r}\frac{[\mathrm{L}_i](1+[\mathrm{H}^+]/K_i^{\mathrm{H}}+[\mathrm{Mg}^{2+}]/K_i^{Mg})}{K_i^K\left(P_i([\mathrm{H}^+],[\mathrm{Mg}^{2+}],[\mathrm{K}^+])\right)^2}. \tag{2.47}$$

The flux terms for H^+, Mg^{2+}, and K^+ are

$$\Phi^{\mathrm{H}}=-\sum_{i=1}^{N_r}\frac{\partial[\mathrm{H}_{bound}]}{\partial[\mathrm{L}_i]}\frac{d[\mathrm{L}_i]}{dt}+\sum_{k=1}^{N_f}n_kJ_k+J_t^{\mathrm{H}}, \tag{2.48}$$

$$\Phi^{Mg}=-\sum_{i=1}^{N_r}\frac{\partial[\mathrm{Mg}_{bound}]}{\partial[\mathrm{L}_i]}\frac{d[\mathrm{L}_i]}{dt}+J_t^{Mg}, \tag{2.49}$$

$$\Phi^{K}=-\sum_{i=1}^{N_r}\frac{\partial[\mathrm{K}_{bound}]}{\partial[\mathrm{L}_i]}\frac{d[\mathrm{L}_i]}{dt}+J_t^{K}, \tag{2.50}$$

where N_r is the number of reactants, N_f is the number of reactions, n_k is the stoichiometric coefficient of the kth reaction, J_k is the flux of the kth reaction, and $J_t^H(J_t^{Mg}, J_t^K)$ is the transport flux of $[H^+]([Mg^{2+}], [K^+])$ into the system.

The buffering terms are

$$\alpha_{\mathrm{H}}=1+\frac{\partial[\mathrm{H}_{bound}]}{\partial[\mathrm{H}^+]}, \tag{2.51}$$

$$\alpha_{Mg}=1+\frac{\partial[\mathrm{Mg}_{bound}]}{\partial[\mathrm{Mg}^{2+}]}, \tag{2.52}$$

$$\alpha_{K}=1+\frac{\partial[\mathrm{K}_{bound}]}{\partial[\mathrm{K}^{+}]}, \tag{2.53}$$

The time derivatives of $[H^+]$, $[Mg^{2+}]$, and $[K^+]$ obtained from solving Eqs. (2.36), (2.37), and (2.38) are given in terms of the buffering terms and the flux terms defined in the preceding equations:

$$\begin{aligned}\frac{d[\mathrm{H}^{+}]}{dt}=&\left[\left(\frac{\partial[\mathrm{K}_{bound}]}{\partial[\mathrm{Mg}^{2+}]}\cdot\frac{\partial[\mathrm{Mg}_{bound}]}{\partial[\mathrm{K}^{+}]}-\alpha_{Mg}\alpha_{K}\right)\Phi^{\mathrm{H}}\right.\\&+\left(\alpha_{K}\frac{\partial[\mathrm{H}_{bound}]}{\partial[\mathrm{Mg}^{2+}]}-\frac{\partial[\mathrm{H}_{bound}]}{\partial[\mathrm{K}^{+}]}\cdot\frac{\partial[\mathrm{K}_{bound}]}{\partial[\mathrm{Mg}^{2+}]}\right)\Phi^{Mg}\\&\left.+\left(\alpha_{Mg}\frac{\partial[\mathrm{H}_{bound}]}{\partial[\mathrm{K}^{+}]}-\frac{\partial[\mathrm{H}_{bound}]}{\partial[\mathrm{Mg}^{2+}]}\cdot\frac{\partial[\mathrm{Mg}_{bound}]}{\partial[\mathrm{K}^{+}]}\right)\Phi^{K}\right]/D,\end{aligned} \tag{2.54}$$

$$\begin{aligned}\frac{d[\mathrm{Mg}^{2+}]}{dt}=&\left[\left(\alpha_{K}\frac{\partial[\mathrm{Mg}_{bound}]}{\partial[\mathrm{H}^{+}]}-\frac{\partial[\mathrm{K}_{bound}]}{\partial[\mathrm{H}^{+}]}\cdot\frac{\partial[\mathrm{Mg}_{bound}]}{\partial[\mathrm{K}^{+}]}\right)\Phi^{\mathrm{H}}\right.\\&+\left(\frac{\partial[\mathrm{K}_{bound}]}{\partial[\mathrm{H}^{+}]}\cdot\frac{\partial[\mathrm{H}_{bound}]}{\partial[\mathrm{K}^{+}]}-\alpha_{\mathrm{H}}\alpha_{K}\right)\Phi^{Mg}\\&\left.+\left(\alpha_{\mathrm{H}}\frac{\partial[\mathrm{Mg}_{bound}]}{\partial[\mathrm{K}^{+}]}-\frac{\partial[\mathrm{H}_{bound}]}{\partial[\mathrm{K}^{+}]}\cdot\frac{\partial[\mathrm{Mg}_{bound}]}{\partial[\mathrm{H}^{+}]}\right)\Phi^{K}\right]/D,\end{aligned} \tag{2.55}$$

$$\begin{aligned}\frac{d[\mathrm{K}^{+}]}{dt}=&\left[\left(\alpha_{Mg}\frac{\partial[\mathrm{K}_{bound}]}{\partial[\mathrm{H}^{+}]}-\frac{\partial[\mathrm{K}_{bound}]}{\partial[\mathrm{Mg}^{2+}]}\cdot\frac{\partial[\mathrm{Mg}_{bound}]}{\partial[\mathrm{H}^{+}]}\right)\Phi^{\mathrm{H}}\right.\\&+\left(\alpha_{\mathrm{H}}\frac{\partial[\mathrm{K}_{bound}]}{\partial[\mathrm{Mg}^{2+}]}-\frac{\partial[\mathrm{K}_{bound}]}{\partial[\mathrm{H}^{+}]}\cdot\frac{\partial[\mathrm{H}_{bound}]}{\partial[\mathrm{Mg}^{2+}]}\right)\Phi^{Mg}\\&\left.+\left(\frac{\partial[\mathrm{Mg}_{bound}]}{\partial[\mathrm{H}^{+}]}\cdot\frac{\partial[\mathrm{H}_{bound}]}{\partial[\mathrm{Mg}^{2+}]}-\alpha_{\mathrm{H}}\alpha_{Mg}\right)\Phi^{K}\right]/D,\end{aligned} \tag{2.56}$$

where

$$\begin{aligned}D=&\alpha_{\mathrm{H}}\frac{\partial[\mathrm{K}_{bound}]}{\partial[\mathrm{Mg}^{2+}]}\cdot\frac{\partial[\mathrm{Mg}_{bound}]}{\partial[\mathrm{K}^{+}]}+\alpha_{K}\frac{\partial[\mathrm{H}_{bound}]}{\partial[\mathrm{Mg}^{2+}]}\cdot\frac{\partial[\mathrm{Mg}_{bound}]}{\partial[\mathrm{H}^{+}]}\\&+\alpha_{Mg}\frac{\partial[\mathrm{H}_{bound}]}{\partial[\mathrm{K}^{+}]}\cdot\frac{\partial[\mathrm{K}_{bound}]}{\partial[\mathrm{H}^{+}]}-\alpha_{Mg}\alpha_{K}\alpha_{\mathrm{H}}\\&-\frac{\partial[\mathrm{H}_{bound}]}{\partial[\mathrm{K}^{+}]}\cdot\frac{\partial[\mathrm{K}_{bound}]}{\partial[\mathrm{Mg}^{2+}]}\cdot\frac{\partial[\mathrm{Mg}_{bound}]}{\partial[\mathrm{H}^{+}]}\\&-\frac{\partial[\mathrm{H}_{bound}]}{\partial[\mathrm{Mg}^{2+}]}\cdot\frac{\partial[\mathrm{Mg}_{bound}]}{\partial[\mathrm{K}^{+}]}\cdot\frac{\partial[\mathrm{K}_{bound}]}{\partial[\mathrm{H}^{+}]}.\end{aligned} \tag{2.57}$$

2.4. Multiple cation equilibria in solutions: Proton, magnesium, and potassium ion binding in the creatine kinase reaction

The creatine kinase reaction catalyzes the phosphorylation of ADP by PCr to produce ATP and creatine (Cr). At given pH and free Mg^{2+} and K^+ concentrations, ATP, ADP, PCr, and Cr are distributed as a mixture of different ion bound forms. In a solution with given total amounts of ions and metabolites, the free ion concentrations are determined by the simultaneous binding equilibria of the metabolites with the cations. Experimentally, total concentrations of

metabolites and ions are measured in solution and the free ion concentrations are calculated from ion mass balance equations derived from multiple cation equilibria. Lawson and Veech (1979) determined experimentally the effect of Mg^{2+} and pH on the creatine kinase equilibrium constant at 38 °C by starting with known quantities of either ATP and Cr or PCr and ADP and adding the creatine kinase enzyme to let the reaction proceed to equilibrium. The free magnesium ion concentration was calculated by subtracting total bound magnesium from total magnesium ion concentration. Ionic strength was maintained at 0.25 *M* in these solutions by the addition of almost 250 m*M* of KCl. From the observed equilibrium constants and theoretical calculations, they calculated the creatine kinase apparent equilibrium constant at pH 7, 1 m*M* Mg^{2+}, and 0.25 *M* ionic strength to be 166. This is the number that is often used as the *in vivo* creatine kinase equilibrium constant. However, they did not take potassium binding into account, which was later shown to be comparable to magnesium binding to ATP at physiological concentrations of the potassium ion by Kushmerick (1997). The consequence of not accounting for potassium binding is the underestimation of free magnesium concentration. The ionic strength of I = 0.25 *M* used in these experiments is also very high when compared to values computed from the ionic composition of myoplasm. Godt and Maughan (1988) estimated I = 0.18 *M* for frog myoplasm. Teague and Dobson (1992) studied the effect of temperature on creatine kinase equilibrium experiment under similar conditions as in the Lawson and Veech (1979) study, but varied the temperature. From binding polynomials of metabolites, the reference equilibrium constant was computed at different temperatures. The slope of the plot of log of apparent equilibrium constant versus 1/*T* was used to estimate the reaction enthalpy from the van't Hoff relationship. Subsequent computations of the creatine kinase equilibrium as a function of temperature, Mg^{2+}, and ionic strength (Golding *et al*., 1995; Teague *et al*., 1996) were based on Teague and Dobson (1992) data. Vinnakota (2006) reinterpreted data of Teague and Dobson (1992) with potassium binding in addition to magnesium and proton binding and obtained the values of equilibrium constant and the enthalpy change of the reference reaction.

The reference reaction for the creatine kinase reaction is written in terms of its most deprotonated species in the physiological pH range:

$$HPCr^{2-}+ADP^{3-}+H^{+} \rightleftarrows HCr^{0}+ATP^{4-}. \tag{2.58}$$

The biochemical reaction is written in terms of sums of species as they exist in solution governed by their individual equilibria with protons, magnesium, and potassium ions:

$$PCr+ADP \rightleftarrows ATP+Cr. \tag{2.59}$$

Table 2.2 lists the binding reactions, *pK* values, and dissociation enthalpies for each metabolite in the experimental system of Teague and Dobson (1992).

The concentrations of free magnesium and potassium ions are calculated by solving ion mass conservation relation equations at a given pH:

$$\begin{aligned}[Mg^{2+}_{total}]=&[Mg^{2+}]+[MgATP^{2-}]+2[Mg_2ATP]+[MgHATP^{-}]\\&+[MgADP^{-}]+[Mg_2ADP^{+}]+[MgHPCr]+[MgHPi]\\&+[MgH_2Pi^{+}]\end{aligned} \tag{2.60}$$

$$[K^+_{total}]=[K^+]+[KATP^{3-}]+[KADP^{2-}]+[KHPCr^-]+[KHPi^-]. \tag{2.61}$$

At each temperature, Teague and Dobson's (1992) data give the final equilibrium composition in terms of total Mg^{2+} and K^+ concentrations, total ATP, ATP, PCr and Cr concentrations, and the final pH. We treat the measured final pH as the negative logarithm of $[H^+]$ activity ($-\log_{10}(\gamma[H^+])$) and compute the $[H^+]$ concentration and pH as $-\log_{10}([H^+])$ using an approximate activity coefficient γ calculated from the extended Debye-Huckel equation (Alberty, 2003). Phosphate was added to the medium as one of the buffers. Therefore, phosphate binding to ions is accounted in the overall ion mass balance.

The apparent equilibrium constant of the creatine kinase reaction is given by

$$K^{CK}_{app}=\frac{[ATP]_{eq}\cdot[Cr]_{eq}}{[PCr]_{eq}\cdot[ADP]_{eq}} =\frac{([ATP^{4-}]_{eq}+[HATP^{3-}]_{eq}+[MgATP^{2-}]_{eq}+[MgHATP^-]_{eq}+[Mg_2ATP]_{eq}+[KATP^{3-}]_{eq})([HCr]_{eq}+[H_2Cr^+]_{eq})}{([ADP^{3-}]_{eq}+[HADP^{2-}]_{eq}+[MgADP^-]_{eq}+[Mg_2ADP^+]_{eq}+[KADP^{2-}]_{eq})([HPCr^{2-}]_{eq}+[H_2PCr^-]_{eq}+[MgHPCr]_{eq}+[KHPCr^-]_{eq})} \tag{2.62}$$

Each species of a metabolite can be expressed in terms of the most unbound species through ionic equilibrium relationships defined by binding reactions in Table 2.2. For example, ATP^{4-} is given by

$$[ATP^{4-}]_{eq}=\frac{[ATP]_{eq}}{1+\frac{[H^+]}{K_{HATP}}+\frac{[Mg^{2+}]}{K_{MgATP}}+\frac{[H^+][Mg^{2+}]}{K_{HATP}K_{MgHATP}}+\frac{[Mg^{2+}]^2}{K_{MgATP}K_{Mg2ATP}}+\frac{[K^+]}{K_{KATP}}}. \tag{2.63}$$

The denominator of the RHS of Eq. (2.63) is known as the binding polynomial (P_{ATP}) for ATP:

$$P_{ATP}=1+\frac{[H^+]}{K_{HATP}}+\frac{[Mg^{2+}]}{K_{MgATP}}+\frac{[H^+][Mg^{2+}]}{K_{HATP}K_{MgHATP}} +\frac{[Mg^{2+}]^2}{K_{MgATP}K_{Mg2ATP}}+\frac{[K^+]}{K_{KATP}}. \tag{2.64}$$

Therefore, $[ATP]_{eq} = [ATP^{4-}]_{eq} P_{ATP}$. Similarly, other metabolite concentrations can be expressed in terms of their most unbound forms and binding polynomials. From Eqs. (2.62), (2.63), and (2.64), the apparent equilibrium constant of creatine kinase reaction can be expressed as

$$K^{CK}_{app}=\frac{[ATP^{4-}]_{eq}[HCr]_{eq}}{[HPCr^{2-}]_{eq}[ADP^{3-}]_{eq}[H^+]}[H^+]\frac{P_{ATP}P_{Cr}}{P_{PCr}P_{ADP}}=K^{CK}_{ref}[H^+]\frac{P_{ATP}P_{Cr}}{P_{PCr}P_{ADP}}. \tag{2.65}$$

Binding equilibria were corrected to experimental ionic strength and temperature using the methods described in Section 2.3.1. These constants are also corrected to experimental temperatures using the van't Hoff relationship. We analyzed the equilibrium compositions of solutions in Teague and Dobson's study to compute the reference equilibrium constant of creatine kinase plotted as a function of $1/T$ in Fig. 2.1. From our analysis, we estimate the equilibrium constant of the reference reaction, K^{CK}_{ref}, to be 9.82e8 at 298.15 K and 0.25 *M* ionic

strength, whereas the value of this constant was estimated to be 3.77e8 by Teague and Dobson (1992). From the slope of the plot in Fig. 2.1, we estimate the enthalpy of the reference reaction to be −17.02 ± 3.32 kJ/mol as opposed to the estimate of −16.73 kJ/mol by Teague and Dobson (1992).

After estimating the K_{ref}^{CK}, we then compute the apparent equilibrium constant of the creatine kinase reaction as a function of pH at physiological conditions found in muscle, that is, 310.15 K, 0.18 *M* ionic strength, 1 m*M* free magnesium (Konishi, 1998), and 140 m*M* free potassium (Kushmerick, 1997)(Fig. 2.2). At pH 7 the apparent equilibrium constant under physiological conditions is 166.2. This is very close to the previous estimates of 166 by Lawson and Veech (1979) and Teague and Dobson (1992) at $-\log_{10}(\gamma[H^+]) = 7$ under unphysiological experimental conditions at a high potassium concentration and a high ionic strength. Errors in the analyses by Lawson and Veech (1979) and Teague and Dobson (1992)(ignoring potassium binding and underestimating free magnesium ion concentration and the effect of high ionic strength) tended to cancel out, resulting in an estimate of K_{app}^{CK} at $-\log_{10}(\gamma[H^+]) = 7$ similar to ours at pH 7. Under the experimental conditions of the previous studies (Lawson and Veech, 1979; Teague and Dobson, 1992), that is, 0.25 *M* ionic strength and 250 m*M* K^+ concentration, we compute the apparent equilibrium constant at pH 7 to be 99.3, which is very low compared to the physiological value.

2.5. Example of detailed kinetics of a biochemical reaction: Citrate synthase

Here we present details of modeling a single-reaction system—citrate synthase—applying the principles detailed in the preceding sections. The biochemical reaction is

$$\text{oxaloacetate} + \text{acetyl} - \text{CoA} \rightleftarrows \text{coenzyme A} + \text{citrate}. \tag{2.66}$$

If we denote the flux of this reaction as a function of reactant concentrations by the variable *J*, then the concentration kinetics of the reactants is governed by the differential equation:

$$\begin{aligned} d[\text{oxaloacetate}]/dt &= -J \\ d[\text{acetyl} - \text{CoA}]/dt &= -J \\ d[\text{coenzyme A}]/dt &= +J \\ d[\text{citrate}]/dt &= +J. \end{aligned} \tag{2.67}$$

What remains is to impose an appropriate mathematical expression for *J* that effectively models the kinetics of the reaction in Eq. (2.66). Such expressions are the domain of enzyme kinetics, in which mechanisms are proposed and data are fit to obtain estimates of associated parameters. In searching the literature, we are likely to discover that the existing kinetic models for the enzyme are parameterized from *in vitro* experiments conducted at nonphysiological pH, ionic strength, and $[Mg^{2+}]$. Furthermore, the given mechanism will either violate the Haldane constraint or, if it does not, obey the constraint with a value of the apparent equilibrium constant that matches the nonphysiological conditions of the *in vitro* assay. Accounting and correcting for these facts require treating the detailed biochemical thermodynamics of the reaction system.

To do this we, define reactions in terms of the reference stoichiometry, which in contrast to the biochemical reaction of Eq. (2.66) conserves mass (in terms of elements) and charge:

$$OAA^{2-} + ACCOA^{0} + H_2O \rightleftharpoons COAS^{-} + CIT^{3-} + 2H^{+}. \tag{2.68}$$

Reference species associated with reactants in Eq. (2.66) are listed in Table 2.3. A thermodynamically balanced model for the kinetics of this reaction relies on a calculation of the thermodynamic properties of the reaction. Using data in Table 2.3, the thermodynamic properties are computed:

$$\begin{aligned}\Delta_r G^o &= \Delta_f G^o_{COASH} + \Delta_f G^o_{CIT} - \Delta_f G^o_{OAA} - \Delta_f G^o_{ACCOA} - \Delta_f G^o_{H_2O} \\ &= +42.03\,\mathrm{kJ/mol},\end{aligned} \tag{2.69}$$

$$K^{CS}_{app} = e^{-\Delta_r G'^o/RT} = \frac{P_{COA}\cdot P_{CIT}}{P_{OAA}\cdot P_{ACCOA}\cdot (10^{-\mathrm{pH}})^2} e^{-\Delta_r G^o/RT}, \tag{2.70}$$

where K^{CS}_{app} is the apparent equilibrium constant for the reaction of Eq. (2.66). In other words, in chemical equilibrium $([\mathrm{CoA}][\mathrm{citrate}])/([\mathrm{oxaloacetate}][\mathrm{acetyl-CoA}]) = K^{CS}_{app}$, where these concentrations correspond to sums over all species associated with each reactant. The binding polynomials in Eq. (2.71) depend on pH and binding ion concentration through the following relationships:

$$\begin{aligned}&P_{OAA} = 1 + [\mathrm{Mg}^{2+}]/K_{Mg,OAA}, \\ &P_{CIT} = 1 + 10^{-\mathrm{pH}}/K_{\mathrm{H},CIT} + [\mathrm{Mg}^{2+}]/K_{Mg,CIT} + [\mathrm{K}^{+}]/K_{K,CIT} \\ &P_{ACCOA} = 1,\ P_{COASH} = 1 + 10^{-\mathrm{pH}}/K_{\mathrm{H},COASH}\end{aligned} \tag{2.71}$$

Setting pH = 7, $[\mathrm{K}^+]$ = 150 m*M*, and $[\mathrm{Mg}^{2+}]$ = 1 m*M*, we obtain the apparent thermodynamic properties:

$$\begin{aligned}&\Delta_r G'^o = -47.41\,\mathrm{kJ}\cdot\mathrm{mol}^{-1} \\ &K^{CS}_{app} = 2.02\times 10^8.\end{aligned} \tag{2.72}$$

The relationships between the reference species concentrations and the reactant concentrations are

$$\begin{aligned}&[\mathrm{OAA}^{2-}] = [\mathrm{OAA}]/P_{OAA} \\ &[\mathrm{ACCOA}^{0}] = [\mathrm{ACCOA}]/P_{ACCOA} \\ &[\mathrm{CIT}^{3-}] = [\mathrm{CIT}]/P_{CIT} \\ &[\mathrm{COAS}^{-}] = [\mathrm{COASH}]/P_{COASH}.\end{aligned} \tag{2.73}$$

The computed species concentrations and thermodynamic values are used in the kinetic model of this enzyme.

The enzyme kinetic flux, which is based on a compulsory-order ternary-complex mechanism,

$$\begin{gathered}
\mathrm{E}+\mathrm{OAA}^{2-}\underset{k_{21}}{\overset{k_{12}}{\rightleftharpoons}}\mathrm{E}\cdot\mathrm{OAA}^{2-}\\
\mathrm{E}\cdot\mathrm{OAA}^{2-}+\mathrm{ACCOA}^{0}\underset{k_{32}}{\overset{k_{23}}{\rightleftharpoons}}\mathrm{E}\cdot\mathrm{OAA}^{2-}\cdot\mathrm{ACCOA}^{0}.\\
\mathrm{E}\cdot\mathrm{OAA}^{2-}\cdot\mathrm{ACCOA}^{0}+\mathrm{H_2O}\underset{k_{43}}{\overset{k_{34}}{\rightleftharpoons}}\mathrm{E}\cdot\mathrm{CIT}^{3-}+\mathrm{COAS}^{-}+2\mathrm{H}^{+}\\
\mathrm{E}\cdot\mathrm{CIT}^{3-}\underset{k_{14}}{\overset{k_{41}}{\rightleftharpoons}}\mathrm{E}+\mathrm{CIT}^{3-}
\end{gathered} \tag{2.74}$$

where E denotes the enzyme and is tested and parameterized against experimental data in Beard *et al*. (2008). In addition to treating the enzyme kinetic mechanism explicitly in terms of biochemical species, the Beard *et al*. (2008) model also accounts for pH dependence of enzyme activity by treating the enzyme as a monobasic acid with the unbound form of the enzyme as the active form. The following expression for V_{max} as a function of $[H^+]$ concentration accounts for the pH dependence of enzyme activity:

$$V_{max}=\frac{V_{max}^{opt}}{1+\frac{[\mathrm{H}^+]}{K_{iH}}}, \tag{2.75}$$

where V_{max}^{opt} is the maximum enzyme velocity attained when all of the enzyme is unbound and K_{iH} is the proton dissociation constant.

3. Application to Physiological Systems

3.1. pH dynamics and glycogenolysis in cell free reconstituted systems and in skeletal muscle

Intracellular pH is an important physiological variable that is regulated within a narrow range. The preceding sections showed that pH significantly affects enzyme activities and apparent equilibrium constants of biochemical reactions. These in turn may influence the energetic state of muscle and the metabolic fluxes. Computational models of biochemical pathways with the capability to predict the metabolic proton load and the consequent changes in muscle pH are useful tools for investigating pH regulation during physiological situations such as exercise and pathological conditions such as ischemia/reperfusion. The models of glycogenolysis developed by Vinnakota (2006) and Vinnakota *et al*. (2006) compute the metabolic proton load due to glycogenolysis in isolated cell free reconstituted systems and in intact mouse skeletal muscle during anoxia/reperfusion. Vinnakota *et al*. (2006) considered H^+, Mg^{2+}, and K^+ ion binding to the metabolites in the pathways modeled. However, the K^+ concentration was kept constant because of its low relative change during the transients modeled.

Scopes (1974) simulated postmortem glycogenolysis in a reconstituted system with rabbit and porcine enzymes from the glycogenolysis pathway, breaking down glycogen into lactate. ATPase and AMPdeaminase were added to this system with an initial concentration of PCr at 24 m*M* and an initial pH of 7.25. Figures 2.3 and 2.4 show pH time course data and model simulation and the computed proton generation fluxes due to biochemical reactions from the study of Vinnakota *et al*. (2006). The pH time course shows a slight initial rise in pH and thereafter a nearly linear decline until a final pH is reached near 5.5 at 190 min that continues until 300 min. The proton fluxes due to CK, ATPase, glycogenolysis, and AMP deaminase are plotted along with the sum total of all fluxes in Fig. 2.4. These fluxes identify the role of each biochemical reaction in shaping the pH transient. The creatine kinase flux initially consumes protons, which explains the initial rise in pH. The sum of proton fluxes due to the ATPase

reaction and the glycogenolysis pathway has a flat time course, which explains the nearly linear decline of pH from 20 to 190 min. However, the important features that emerge from these computations are that (1) the ATPase proton flux is acidifying in the physiological pH range 7.2—6.8 and (2) the contribution of proton fluxes from the glycogenolysis pathway is relatively small during this pH range. The sharp decline in glycogenolysis at the end is due to a reduction in glycogen and a degradation of the adenine nucleotide pool. In summary, near-normal resting pH ATP hydrolysis is the source of metabolic acid load during anaerobic glycogenolysis. However, it is important to note that proton stoichiometries of biochemical reactions are variable with pH, which means that ATP hydrolysis is not always acidifying and that the combined proton stoichiometry of all biochemical reactions in the pathway breaking down glycogen into lactate is not always slightly alkalinizing at all pH values. These results are important for computing metabolic acid load during ischemia and anoxia in cardiac and skeletal muscle, where oxidative ATP generation is impaired, and the creatine kinase and the ATP generation from glycogenolysis work toward maintaining energy balance. Calculations following the principles outlined here provide mechanistic and accurate answers to continued discussions in the physiological literature on the source of protons in muscle glycogenolysis and glycolysis.

3.2. Cardiac energetics

The heart in healthy mammals is a highly oxidative organ in which normal function is tightly coupled with energetic state, which is maintained by a continuous supply of substrates to fuel energy metabolism (Katz, 2006). When under stresses or disease, such as ischemia or chronic heart failure, impaired cardiac function is associated with the altered energetic state of the heart (Ingwall and Weiss, 2004; Stanley *et al*., 2005; Zhang *et al*., 1993, 2001).

3.2.1. The gibbs free energy of ATP hydrolysis in the heart—The Gibbs free energy of ATP hydrolysis reaction, $\Delta_r G_{ATPase}$, represents an effective marker of the cardiac energetic state. Based on the chemical reference reaction of the ATP hydrolysis,

$$\mathrm{ATP^{4-}+H_2O=ADP^{3-}+PI^{2-}+H^+}, \tag{2.76}$$

the standard Gibbs free energy of ATP hydrolysis, $\Delta_r G^o_{ATPase}$, can be calculated from Eq. (2.3) as

$$\Delta_r G^o_{ATPase}=\Delta_f G^o_{ADP}+\Delta_f G^o_{PI}+\Delta_f G^o_{\mathrm{H}}-\Delta_f G^o_{ATP}-\Delta_f G^o_{\mathrm{H2O}}, \tag{2.77}$$

with the corresponding equilibrium constant

$$K^{ATPase}_{ref}=\exp\left(-\frac{\Delta_r G^o_{ATPase}}{RT}\right)=\left(\frac{[\mathrm{ADP^{3-}}]_c[\mathrm{PI^{2-}}][\mathrm{H^+}]}{[\mathrm{ATP}]^{4-}}\right)_{eq}. \tag{2.78}$$

For the biochemical reaction of ATP hydrolysis,

$$\mathrm{ATP=ADP+PI}, \tag{2.79}$$

the transformed equilibrium constant and standard Gibbs free energy can be calculated as

$$\mathrm{K}_{app}^{ATPase}=\left(\frac{[\mathrm{ADP}][\mathrm{PI}]}{[\mathrm{ATP}]}\right)_{eq}=\frac{K_{ref}^{ATPase}}{[\mathrm{H}^{+}]}\frac{P_{ADP}P_{PI}}{P_{ATP}}, \tag{2.80}$$

and

$$\Delta_r G'^{\mathrm{o}}_{\mathrm{ATPase}}=-\mathrm{RT}\ln K_{app}^{ATPase}, \tag{2.81}$$

where P_{ATP}, P_{ADP}, and P_{PI} are the binding polynomials as functions of ionic concentrations (e.g., $[\mathrm{H}^+]$, $[\mathrm{Mg}^{2+}]$, and $[\mathrm{K}^+]$) and $\Delta_r G_{ATPase}$ is obtained from the definition stated in Eq. (2.2),

$$\Delta_r G_{ATPase}=\Delta_r G'^{o}_{ATPase}+RT\ln\left(\frac{[\mathrm{ADP}][\mathrm{PI}]}{[\mathrm{ATP}]}\right). \tag{2.82}$$

3.2.2. Calculations of $\Delta_{\mathrm{r}}G'^{o}_{ATPase}$ and ΔG_{ATPase} in the heart *in vivo*—Cardiomyocytes contain multiple subcellular organelles (Katz, 2006), including myofibrils, mitochondria, sarcoplasmic reticulum, and nuclei, among which myofibrils and mitochondria occupy the largest fractions of intracellular volume (Vinnakota and Bassingthwaighte, 2004). Most metabolites and ions require specific protein carriers to traverse the inner mitochondrial membrane (LaNoue and Schoolwerth, 1979; Nelson and Cox, 2005), which constitutes a compartment. To account for this compartmentation, we divide the cellular volume of cardiomyocytes into cytoplasm and mitochondria, where the local concentrations of metabolites drive local biochemical reactions. The free energies for a biochemical reaction are generally different in different intracellular compartments (Gibbs, 1978). Since most of the most energy-consuming processes coupled to ATP hydrolysis, such as mechanical contraction due to myosin ATPase, calcium handling, and maintenance of ion gradients across the sarcolemma, are located in the cytoplasm, the cytoplasmic $\Delta_r G_{ATPase}$ provides the driving force for normal cardiac function (Gibbs, 1985).

Under the physiological conditions with assumed temperature T = 310.15 K, ionic strength I = 0.17 *M*, $\mathrm{pH_c}$ = 7.1, $[\mathrm{Mg}^{2+}]_{\mathrm{c}}$ = 1 m*M*, and $[\mathrm{K}^+]_{\mathrm{c}}$ = 130 m*M*, we are able to compute $\Delta G'^{\mathrm{o}}_{\mathrm{eq,ATPase}}=-34.7\ \mathrm{kJ\ mol^{-1}}$ in the cytoplasm of the cardiomyocytes based on thermodynamic data listed in Table 2.2. Here the subscript "c" denotes cytoplasm. A more detailed process for estimating $\Delta G'^{\mathrm{o}}_{\mathrm{eq,ATPase}}$ is given later.

3.2.3. Example 1: Calculating cytoplasmic $\Delta_r G'^{o}_{ATPase}$ in the heart under *in vivo* physiological conditions—Step 1: Based on basic thermodynamic data and computational algorithm presented elsewhere (Alberty, 2003; Beard and Qian, 2007; Golding *et al*., 1995; Teague *et al*., 1996), K_{ref}^{ATPase} under the physiological conditions (T = 310.15 K and I = 0.17 *M*) is calculated to be $1.16-10^{-1}$.

Step 2: Using the binding constants presented in Table 2.2, we can calculate the binding polynomials under the environmental conditions and cytoplasmic ion concentrations to be P_{ADP} = 2.82, P_{PI} = 1.58, and P_{ATP} = 9.28, respectively.

Step 3: From Eq. (2.80),

$$K_{app}^{ATPase}=\left(\frac{[\mathrm{ADP}][\mathrm{PI}]}{[\mathrm{ATP}]}\right)_{eq}=\frac{K_{ref}^{ATPase}}{[\mathrm{H}^+]_c}\frac{P_{ADP}P_{PI}}{P_{ATP}}=7.03\times10^5. \tag{2.83}$$

Step 4: From Eq. (2.81),

$$\Delta_r G'^{o}_{ATPase}=-RT\ln K_{app}^{ATPase}=-34.72\ \mathrm{kJ\ mol^{-1}}. \tag{2.84}$$

3.2.4. Example 2: Calculating $\Delta_r G_{ATPase}$ at basal work rate in the heart *in vivo*

—The values of basal $[ATP]_c$, $[ADP]_c$, and $[PI]_c$ are 9.67×10^{-3}, 4.20×10^{-5}, and 2.90×10^{-4} *M*, respectively, as reported previously (Wu *et al*., 2008). Thus,

$$\begin{aligned}\Delta_r G_{ATPase}&=\Delta_r G'^{o}_{ATPase}+RT\ln\left(\frac{[\mathrm{ADP}][\mathrm{PI}]}{[\mathrm{ATP}]}\right)\\&=-34.7+2.58\times(-13.6)=-69.8\ \mathrm{kJ\ mol^{-1}}.\end{aligned} \tag{2.85}$$

[Note that in Wu *et al*.2008 this value was reported as −70.0 kJ mol $^{-}{}_{1}$ because $\Delta_r G'^{o}_{ATPase}$ was computed based on slightly different dissociation constants.] A previous computational analysis (Wu *et al*., 2008) showed that $\Delta_r G_{ATPase}$ changes from −70 kJ mol^{-1} at the basal work rate to −64 kJ mol^{-1} at the maximal work rate in the normal dog heart *in vivo*, which means that the threefold of work increase results in an increase of around 2.5 RT in $\Delta_r G_{ATPase}$. The values of $\Delta_r G_{ATPase}$ over the threefold increase of workload are calculated by assuming pH_c, $[Mg^{2+}]_c$, and $[K^+]_c$ fixed at the basal values.

3.2.5. Effects of changes in ion concentrations on $\Delta_r G'^{o}$ of biochemical reactions in the mitochondrial matrix—

The preceding sections showed that the standard free energy of a biochemical reaction is a function of the binding polynomials of the biochemical reactants and is therefore dependent on free ion concentrations. In the mitochondrial matrix, the temporal changes in free ion concentrations are determined by ion transport fluxes across the mitochondrial inner membrane and the ion fluxes are due to biochemical reactions. The differential equations for the time derivatives of ion concentrations derived based on the principles and methods described in the preceding sections are presented in detail elsewhere (Beard and Qian, 2007; Vinnakota, 2006). Figure 2.5 shows the changes in ion concentrations in the mitochondrial matrix (A) and the resulting changes in standard free energies of selected biochemical reactions (B). In Fig. 2.5A, steady-state values of $[H^+]_{matrix}$, $[Mg^{2+}]_{matrix}$, and $[K^+]_{matrix}$ are plotted against an increased *in vivo* cardiac work rate, that is, oxygen consumption rate (MVO_2). As MVO_2 increases from its baseline workload value [3.5 μmol min^{-1} (g tissue)$^{-1}$] to its maximal workload value [10.7 μmol min^{-1} (g tissue)$^{-1}$], $[H^+]_{matrix}$ increases from 5.77×10^{-7} to 6.12×10^{-8} *M*, $[Mg^{2+}]_{matrix}$ decreases from 1.18 to 0.80×10^{-3} *M*, and $[K^+]_{matrix}$ increases from 9.45×10^{-2} to 1.00×10^{-1} *M*, respectively. Since the K^+/H^+ antiporter on the inner mitochondrial membrane is operated near equilibrium in the computational model (Wu *et al*., 2007b), the increase of $[K^+]_{matrix}$ is almost linearly proportional to that of $[H^+]_{matrix}$. Figure 2.5B shows that changes in $[H^+]_{matrix}$, $[Mg^{2+}]_{matrix}$, and $[K^+]_{matrix}$ impact the values of $\Delta_r G'^{o}$ of mitochondrial ATP hydrolysis (ATPase), α-ketoglutarate dehydrogenase (AKGD), and citrate synthase (CITS) differently over the range of the *in vivo* work rate. When the workload is elevated from the baseline value to the maximal

value, $-\Delta_r G'^o_{ATPase}/RT$ decreases from 20.70 to 19.77, $-\Delta_r G'^o_{AKGD}/RT$ decreases from 15.47 to 15.42, and $\Delta_r G'^o_{CITS}/RT$ decreases from 20.46 to 20.15. $\Delta_r G'^o_{ATPase}$ changes the most by around 1 RT unit (i.e., 2.58 kJ mol^{-1}), which means that the apparent equilibrium constant of the mitochondrial ATP hydrolysis varies around threefold. For a biochemical reaction operating near equilibrium, the ratio of forward and reverse reaction fluxes is closely coupled to changes in the apparent equilibrium constants via the mass action law (Beard and Qian, 2007). Equation (81) shows that a small change in $\Delta_r G'^o_{ATPase}$ results in a large change in K_{app}^{ATPase} due to exponentiation. For example, the reaction catalyzed by aconitase in the citric acid cycle, which converts citrate into isocitrate, is maintained near equilibrium under physiological conditions (Wu *et al*., 2007b) with $\Delta_r G'^o_{ACON}$=9.42kJ mol^{-1} at the baseline work rate and $\Delta_r G'^o_{ACON}$=8.99kJ mol^{-1} at the maximal work rate. The decrease of $\Delta_r G'^o_{ACON}$ by 0.43 kJ mol^{-1} leads to the increase of corresponding K_{app}^{ACON} by about 18 %.

3.3. Physiological significance of multiple ion binding equilibria, reaction kinetics, and thermodynamics in cardiac energetics

The advantages of accounting for multiple ion binding equilibria, reaction kinetics, and thermodynamics are demonstrated in recent cardiac energetics studies by Wu *et al*. (2007b, 2008). As shown in Wu *et al*. (2007b), the enzyme mechanisms are presented in terms of chemical species, $\Delta_r G'^o$ of the biochemical reactions are computed by explicitly accounting for effects of ion concentrations, and the corresponding apparent equilibrium constants are used to establish the Haldane constraints for modeling the enzyme kinetics. Accurate estimation of the free energy of ATP hydrolysis is important for determining the energetic state of the heart under various conditions.

The application of the methodologies explained in this chapter in a detailed computational model of cardiac energetics (Wu *et al*., 2008) has resulted in the first estimates of free energy of ATP hydrolysis in the heart *in vivo* at rest and during increased workloads that account for intracellular compartmentation. The capability of the heart to maintain its “energy homeostasis” in a wide range of cardiac workloads has been a puzzle since the mid-1980s (Balaban *et al*., 1986). The ^{31}P magnetic resonance spectroscopy (^{31}P-MRS) technique has been applied widely and successfully as a noninvasive technique in studying *in vivo* cardiac energetics, albeit with difficulties in detecting subcellular concentrations of chemical species and low concentrations of phosphate metabolites, such as ADP and resting Pi. Because of these limitations, the ^{31}P-MRS experimental observations may not provide quantitative measurement on concentration changes of certain metabolites (e.g., cytosolic [Pi]) and may lead to an inaccurate estimation of energy states in the heart *in vivo*. Thus, it is necessary to use a computational tool to unambiguously determine the concentrations and energetic states based on the experimental observations. Also, modeling reveals details of the underlying mechanisms that are not amenable to direct experimental observation and quantification.

The model of Wu *et al.* (2008) predicts significant changes in cytosolic [Pi] from the basal work rate to the maximal work rate and leads to two novel conclusions that will be contentious and inspire more thinking and experimenting. The first conclusion is that oxidative phosphorylation is controlled by Pi feedback in the heart *in vivo*; the second conclusion is that decreased ATP hydrolysis potential—caused by increased cytoplasmic Pi and ADP concentrations—limits ATP utilization rates at a high workload and during ischemia. These two hypotheses are supported by agreement between the model predictions and experimental observations on independent experimental data on transient changes and steady states in ischemic heart *in vivo* (Wu *et al*., 2008).

4. Discussion

4.1. Integrating thermodynamic information in biochemical model building

We have described the methods for accounting for detailed thermodynamics in kinetic simulations of biochemical systems. These methods are crucial for a number of applications, including identifying and parameterizing catalytic mechanisms for enzymes based on *in vitro* data and translating from *in vitro* experiments to predicting *in vivo* function of enzymes. In addition, in analyzing *ex vivo* data (such as from purified mitochondria) or simulating extreme *in vivo* states (such as ischemia/hypoxia), even normally irreversible reactions approach or go to equilibrium. Thus it is always important to accurately account for thermodynamics.

Studies of specific enzymes and transporters (Beard *et al*., 2008; Dash and Beard, 2008; Qi *et al*., 2008) have shown that raw data in the literature are very useful because they are consistent and may be explained with consensus mechanistic models. However, the kinetic parameters originally reported based on those raw data are not always consistent. By reanalyzing raw data from several kinetic studies for enzymes and transporters, we have been able to show that data introduced to support competing hypotheses (different mechanisms) are actually consistent with one consensus mechanism for each enzyme or transporter, and obtain associated kinetic parameter estimates. In general, it is necessary to reanalyze reported data and determine a mechanism (or mechanisms) and associated parameter estimates that account for biochemical state and the kinetic data for each enzyme and transporter.

4.2. Databases of biochemical information

Simulation of large-scale systems will require the development of databases of kinetic and thermochemical data from which models can be assembled. Recently developed models of glycolysis (Vinnakota, 2006; Vinnakota *et al*., 2006) and mitochondrial energetics (Wu *et al*., 2007a, b, 2008) have been built in part based on thermodynamic data complied by Alberty (2003). Analysis and simulation of larger scale systems will require extending Alberty's thermodynamic database for species and reactions not currently included and developing and parameterizing mechanistic models for large numbers of enzymes and metabolite transporters.

In addition to data on thermodynamic constants, databases of kinetic mechanisms and parameters are needed. For many enzymes, detailed mechanistic models have been previously developed based on kinetic measurements made using purified enzymes *in vitro.* However, in nearly all cases much work remains to adapt and extend these mechanistic models to account for the biochemical state (pH, ionic strength, etc.) so that each enzyme model may be incorporated into an integrated system model in a rigorous way. Therefore, it will be necessary to collect kinetic mechanisms and associated parameters.

A number of databases on enzyme kinetics currently exist, with BRENDA (www.brenda.uni-koeln.de) being perhaps the most widely recognized. BRENDA is a clearinghouse of a vast amount of information on enzymes, including estimates of functional parameters (i.e., apparent kinetic constants) and pointers to the primary literature. A recent effort called System for the Analysis of Biochemical Pathways (SABIO-RK, sabio. villa-bosch.de) aims to collect kinetic models and data from the literature. While these tools are useful, much more focused and specialized tools are needed as well. Along these lines we have begun construction of a Biological Components Databank (www.biocoda.org) to provide an online clearinghouse of mechanistic models of functional biological components to use as building blocks to construct computational models of biological systems. Here, rather than compiling the reported estimates of kinetic constants obtained from the original sources, we are reanalyzing reported data and determining mechanisms and associated parameter estimates

for a number of enzymes and transporters. As pilot studies, we have gone through this process for several components.

Our goal is to build a data bank where each entry meets detailed validation and mechanistic standards. However, it is important to realize that it is unavoidable that each entry will pose a unique challenge, requiring a critical assessment of the literature and an expert analysis of data. Therefore, building this data bank will be a huge effort, requiring widespread collaboration within the community. Information on how to contribute to the data bank can be found on the Web site.

Acknowledgments

This work supported by NIH grant HL072011.

References

Alberty RA. Levels of thermodynamic treatment of biochemical reaction systems. Biophys J 1993;65:1243–1254. [PubMed: 8241405]

Alberty, RA. Thermodynamics of Biochemical Reactions. Wiley-Interscience; Hoboken, NJ: 2003.

Alberty RA. A short history of the thermodynamics of enzyme-catalyzed reactions. J Biol Chem 2004;279:27831–27836. [PubMed: 15073189]

Alberty RA. Relations between biochemical thermodynamics and biochemical kinetics. Biophys Chem 2006;124:11–17. [PubMed: 16766115]

Balaban RS, Kantor HL, Katz LA, Briggs RW. Relation between work and phosphate metabolite in the *in vivo* paced mammalian heart. Science 1986;232:1121–1123. [PubMed: 3704638]

Beard DA, Qian H. Relationship between thermodynamic driving force and one-way fluxes in reversible processes. PLoS ONE 2007;2:e144. [PubMed: 17206279]

Beard, DA.; Qian, H. Chemical Biophysics: Quantitative Analysis of Cellular Processes. Cambridge Univ. Press; Cambridge, UK: 2008a. Biochemical reaction networks; p. 128-161.

Beard, DA.; Qian, H. Chemical Biophysics: Quantitative Analysis of Cellular Systems. Cambridge Univ. Press; Cambridge, UK: 2008b. Concepts from physical chemistry; p. 7-23.

Beard, DA.; Qian, H. Chemical Biophysics: Quantitative Analysis of Cellular Systems. Cambridge Univ. Press; Cambridge, UK: 2008c. Conventions and calculations for biochemical systems; p. 24-40.

Beard DA, Vinnakota KC, Wu F. Detailed enzyme kinetics in terms of biochemical species: Study of citrate synthase. PLoS ONE 2008;3:e1825. [PubMed: 18350161]

Clarke ECW, Glew DN. Evaluation of Debye-Huckel limiting slopes for water between 0 and 50 C. J Chem Soc Faraday Trans 1 1980;76:1911–1916.

Dash RK, Beard DA. Analysis of cardiac mitochondrial Na^+/Ca^{2+} exchanger kinetics with a biophysical model of mitochondrial Ca^{2+} handing suggests a 3:1 stoichiometry. J Physiol 2008;586:3267–3285. [PubMed: 18467367]

Frieden C, Alberty RA. The effect of pH on fumarase activity in acetate buffer. J Biol Chem 1955;212:859–868. [PubMed: 14353887]

Gibbs C. The cytoplasmic phosphorylation potential: Its possible role in the control of myocardial respiration and cardiac contractility. J Mol Cell Cardiol 1985;17:727–731. [PubMed: 3900424]

Gibbs CL. Cardiac energetics. Physiol Rev 1978;58:174–254. [PubMed: 146205]

Godt RE, Maughan DW. On the composition of the cytosol of relaxed skeletal muscle of the frog. Am J Physiol 1988;254:C591–C604. [PubMed: 3284380]

Golding EM, Teague WE Jr, Dobson GP. Adjustment of K′ to varying pH and pMg for the creatine kinase, adenylate kinase and ATP hydrolysis equilibria permitting quantitative bioenergetic assessment. J Exp Biol 1995;198:1775–1782. [PubMed: 7636446]

Guyton, AC.; Hall, JE. Textbook of Medical Physiology. Elsevier Saunders; Philadelphia: 2006.

Ingwall JS, Weiss RG. Is the failing heart energy starved? On using chemical energy to support cardiac function. Circ Res 2004;95:135–145. [PubMed: 15271865]

Katz, AM. Physiology of the Heart. Lippincott Williams & Wilkins; Philadelphia: 2006.

Konishi M. Cytoplasmic free concentrations of Ca^{2+} and Mg^{2+} in skeletal muscle fibers at rest and during contraction. Japan J Physiol 1998;48:421–438. [PubMed: 10021496]

Korzeniewski B. Theoretical studies on the regulation of oxidative phosphorylation in intact tissues. Biochim Biophys Acta 2001;1504:31–45. [PubMed: 11239483]

Kushmerick MJ. Multiple equilibria of cations with metabolites in muscle bioenergetics. Am J Physiol 1997;272:C1739–C1747. [PubMed: 9176167]

LaNoue KF, Schoolwerth AC. Metabolite transport in mitochondria. Annu Rev Biochem 1979;48:871–922. [PubMed: 38739]

Lawson JW, Veech RL. Effects of pH and free Mg^{2+} on the Keq of the creatine kinase reaction and other phosphate hydrolyses and phosphate transfer reactions. J Biol Chem 1979;254:6528–6537. [PubMed: 36398]

Lineweaver H, Burk D. The determination of enzyme dissociation constants. J Am Chem Soc 1934;56:658–666.

Nelson, DL.; Cox, MM. Lehninger Principles of Biochemistry. W.H. Freeman; New York: 2005.

Qi F, Chen X, Beard DA. Detailed kinetics and regulation of mammalian NAD-linked isocitrate dehydrogenase. Biochim Biophys Acta 2008;1784:1641–1651. [PubMed: 18672100]

Scopes RK. Studies with a reconstituted muscle glycolytic system: The rate and extent of glycolysis in simulated post-mortem conditions. Biochem J 1974;142:79–86. [PubMed: 4280304]

Stanley WC, Recchia FA, Lopaschuk GD. Myocardial substrate metabolism in the normal and failing heart. Physiol Rev 2005;85:1093–1129. [PubMed: 15987803]

Teague WE Jr, Dobson GP. Effect of temperature on the creatine kinase equilibrium. J Biol Chem 1992;267:14084–14093. [PubMed: 1629208]

Teague WE Jr, Golding EM, Dobson GP. Adjustment of K′ for the creatine kinase, adenylate kinase and ATP hydrolysis equilibria to varying temperature and ionic strength. J Exp Biol 1996;199:509–512. [PubMed: 8930003]

Vendelin M, Kongas O, Saks V. Regulation of mitochondrial respiration in heart cells analyzed by reaction-diffusion model of energy transfer. Am J Physiol Cell Physiol 2000;278:C747–C764. [PubMed: 10751324]

Vendelin M, Lemba M, Saks VA. Analysis of functional coupling: Mitochondrial creatine kinase and adenine nucleotide translocase. Biophys J 2004;87:696–713. [PubMed: 15240503]

Vinnakota K, Kemp ML, Kushmerick MJ. Dynamics of muscle glycogenolysis modeled with pH time course computation and pH-dependent reaction equilibria and enzyme kinetics. Biophys J 2006;91:1264–1287. [PubMed: 16617075]

Vinnakota, KC. pH Dynamics, Glycogenolysis and Phosphoenergetics in Isolated Cell Free Reconstituted Systems and in Mouse Skeletal Muscle. University of Washington; Seattle, WA: 2006.

Vinnakota KC, Bassingthwaighte JB. Myocardial density and composition: A basis for calculating intracellular metabolite concentrations. Am J Physiol Heart Circ Physiol 2004;286:H1742–H1749. [PubMed: 14693681]

Wu F, Jeneson JA, Beard DA. Oxidative ATP synthesis in skeletal muscle is controlled by substrate feedback. Am J Physiol Cell Physiol 2007a;292:C115–C1247. [PubMed: 16837647]

Wu F, Yang F, Vinnakota KC, Beard DA. Computer modeling of mitochondrial tricarboxylic acid cycle, oxidative phosphorylation, metabolite transport, and electrophysiology. J Biol Chem 2007b; 282:24525–24537. [PubMed: 17591785]

Wu F, Zhang EY, Zhang J, Bache RJ, Beard DA. Phosphate metabolite concentrations and ATP hydrolysis potential in normal and ischemic hearts. J Physiol 2008;586:4193–4208. [PubMed: 18617566]

Zhang J, Merkle H, Hendrich K, Garwood M, From AH, Ugurbil K, Bache RJ. Bioenergetic abnormalities associated with severe left ventricular hypertrophy. J Clin Invest 1993;92:993–1003. [PubMed: 8349829]

Zhang J, Ugurbil K, From AH, Bache RJ. Myocardial oxygenation and high-energy phosphate levels during graded coronary hypoperfusion. Am J Physiol Heart Circ Physiol 2001;280:H318–H326. [PubMed: 11123247]

Zhou L, Stanley WC, Saidel GM, Yu X, Cabrera ME. Regulation of lactate production at the onset of ischaemia is independent of mitochondrial NADH/NAD+: Insights from in silico studies. J Physiol 2005;569:925–937. [PubMed: 16223766]

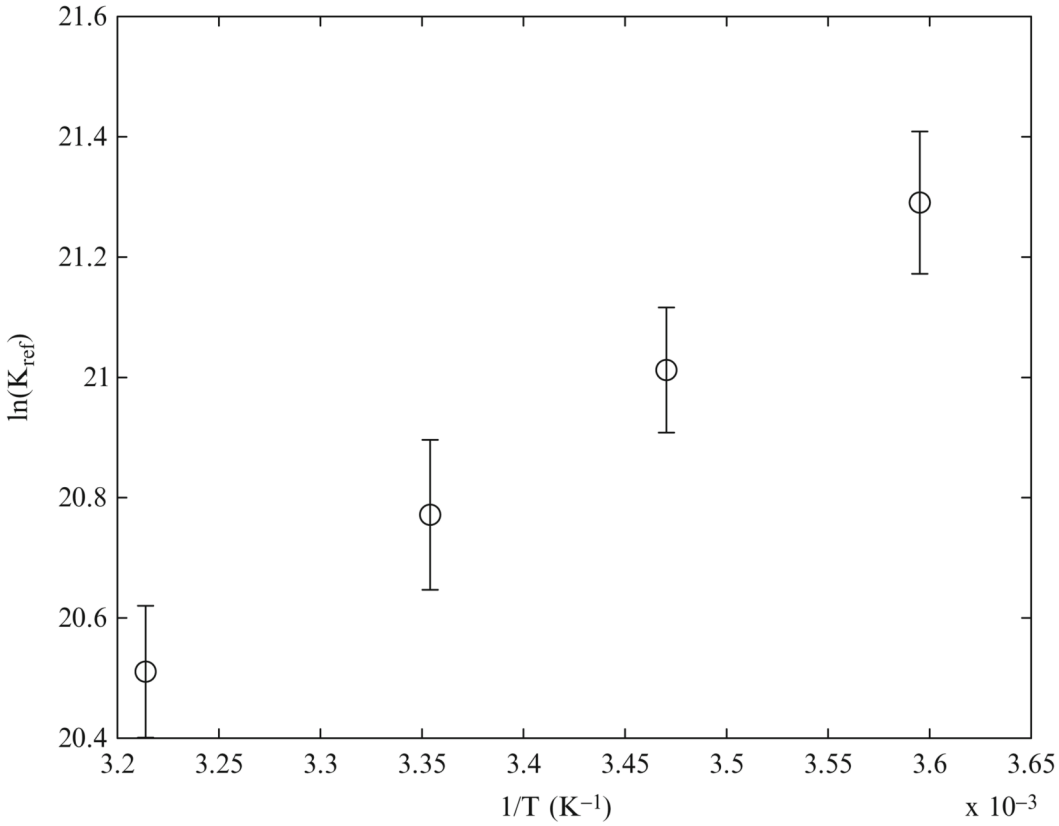

Figure 2.1.
lnK_{ref} of creatine kinase reaction vs 1/T. −R times the slope of this plot gives the enthalpy of the reference reaction.

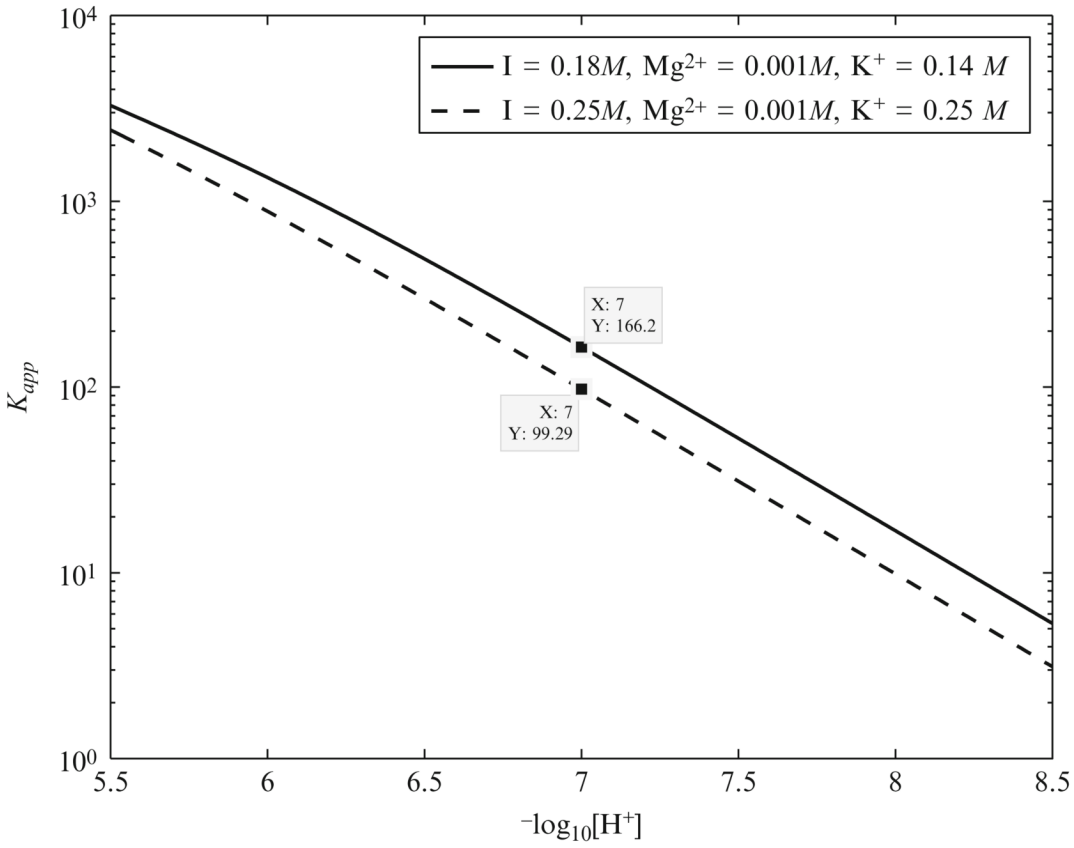

Figure 2.2.

Apparent equilibrium constant of creatine kinase reaction as a function of pH at 310 K, 1 m*M* free magnesium, and two different ionic strength and potassium concentrations: I = 0.18 *M*, K^+ = 140 m*M*; I = 0.25 *M*, K^+ = 250 m*M*.

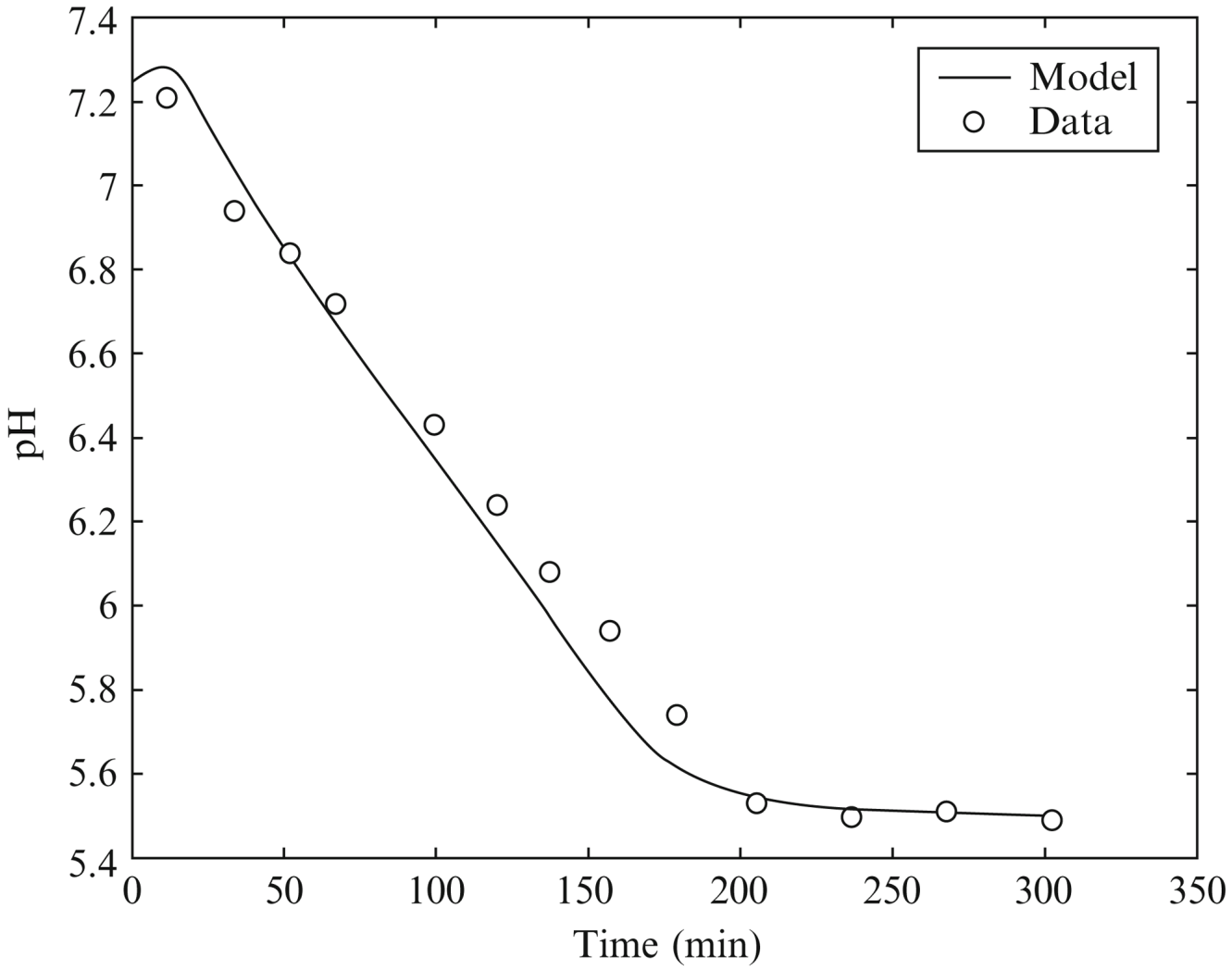

Figure 2.3.
pH transient during simulated postmortem glycogenolysis and model-derived proton fluxes. Reproduced from Vinnakota *et al*. (2006) with permission.

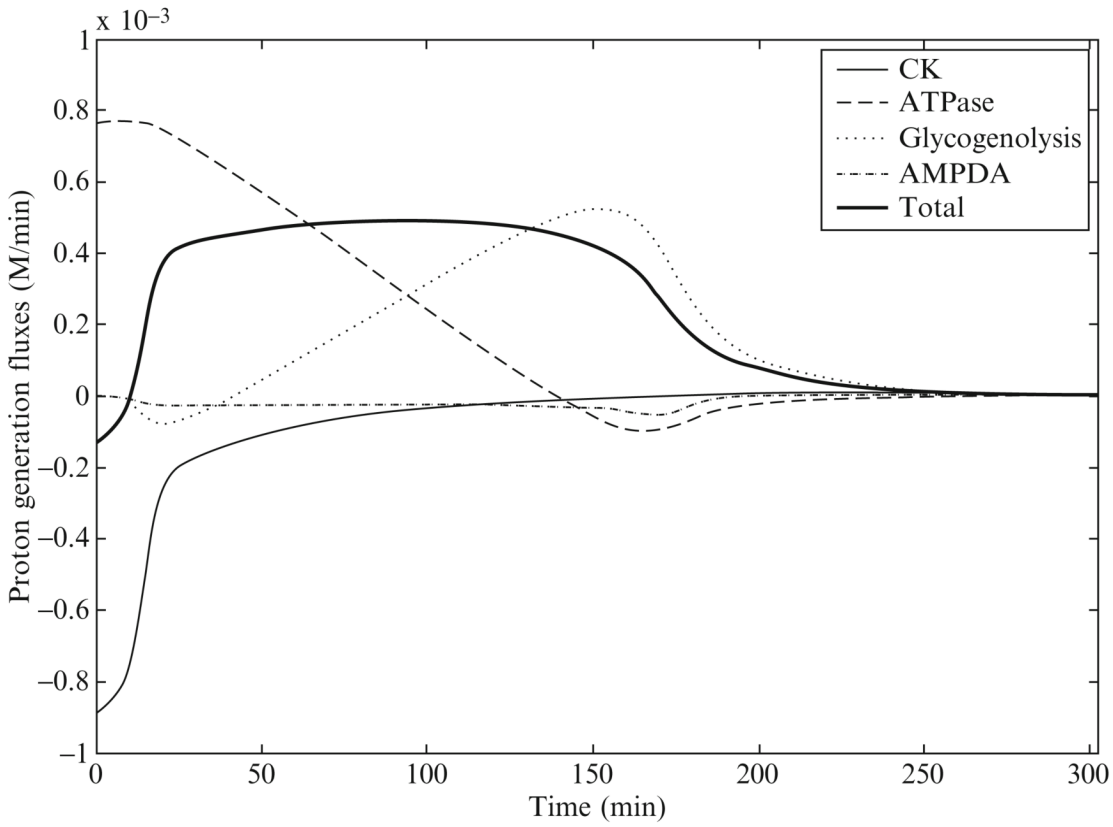

Figure 2.4.
Proton generation fluxes during simulated postmortem glycogenolysis in a cell free reconstituted system. Reproduced from Vinnakota *et al*. (2006) with permission.

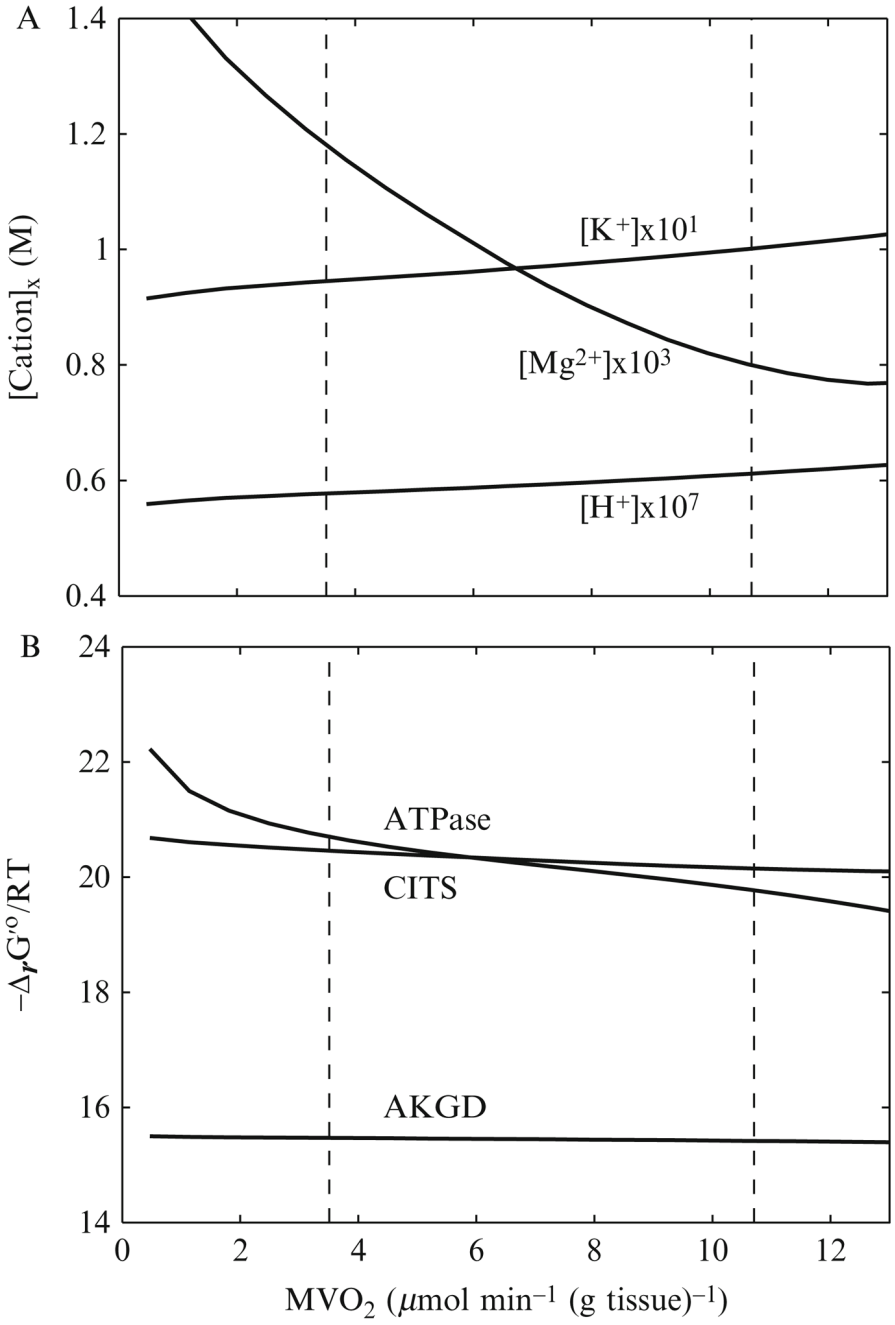

Figure 2.5.

Model-predicted steady-state cation concentrations in the mitochondrial matrix and corresponding $\Delta G'^{o}_{eq}$ of ATP hydrolysis, AKGD, and CITS at various work rates in the heart *in vivo*. (A) Changes in $[H^+]_x$, $[Mg^{2+}]_x$, and $[K^+]_x$, where subscript "x" denotes the mitochondrial matrix. (B) Changes in $\Delta G'^{0}_{ATPase}$ of ATP hydrolysis (ATPase), AKGD, and CITS.

Table 2.1

Terminology

Symbol	Definition	Unit
I	Ionic strength	M
$K_{a,l}$	Dissociation constant for the lth protonation reaction	M
pKa_l	$-\log_{10}(K_{a,l}/c_0)$	Dimensionless
$K_{M,m}$	Dissociation constant for metabolite binding to metal M	M
$pKa_{M,m}$	$-\log_{10}(K_{M,m}/c_0)$	Dimensionless
c_0	Reference concentration for all species (1 M)	M
P_i	Binding polynomial for ith metabolite	Dimensionless
$\overline{N}_H^i$	Average proton binding of ith metabolite at specified T, P, pH, pMg, and I	Dimensionless, noninteger
n_k	Proton generation stoichiometry of the kth reference reaction	Dimensionless
$\Delta_r N_H^k$	Proton generation stoichiometry of the kth biochemical reaction at specified T, P, pH, pMg, and I	Dimensionless, noninteger
$N_H(j)$	Number of H atoms in species j	Dimensionless, integer
z_j	Charge on species j	Dimensionless, integer
$\Delta_f G_j^0(I=0)$	Gibbs energy of formation at zero ionic strength of species j	kJ/mol
v_j^k	Stoichiometric coefficient of species j in the kth reference reaction	
K_{ref}^k	Equilibrium constant of kth reference reaction	Dimensionless
$\Delta_r G_k^0$	Standard free energy of kth reference reaction	kJ/mol
K_{app}^k	Apparent equilibrium constant of kth biochemical reaction	Dimensionless
$\Delta_r G'^0_k$	Standard free energy of kth biochemical reaction	kJ/mol
$\Delta_r G_k$	Free energy span of kth biochemical reaction	kJ/mol
$\Delta_r H_j^0$	Standard Enthalpy of jth proton dissociation reaction at a given ionic strength	kJ/mol
J_r^k	Flux through reaction kth biochemical reaction	M/min
$[L_i]$	Concentration of biochemical reactant i	M

Table 2.2

Binding reactions and equilibrium constants

Metabolite	Binding reaction	*pK* (*T* = 298.15*K*, *I* = 0.1)	Δ*H* (*I* = 0) kJ/mol
ATP	$HATP^{3-} \leftrightharpoons ATP^{4-} + H^{+}$	6.48	−5
	$MgATP^{2-} \leftrightharpoons ATP^{4-} + Mg^{2+}$	4.19	−18
	$MgHATP^{2-} \leftrightharpoons HATP^{3-} + Mg^{2+}$	2.32	—
	$Mg_2ATP \leftrightharpoons MgATP^{2-} + Mg^{2+}$	1.7	—
	$KATP^{3-} \leftrightharpoons ATP^{4-} + K^{+}$	1.17	−1
ADP	$HADP^{2-} \leftrightharpoons ADP^{3-} + H^{+}$	6.38	−3
	$MgADP^{-} \leftrightharpoons ADP^{3-} + Mg^{2+}$	3.25	−15
	$Mg_2ADP^{+} \leftrightharpoons MgADP^{-} + Mg^{2+}$	1	—
	$KADP^{2-} \leftrightharpoons ADP^{3-} + K^{+}$	1	—
PCr	$H_2PCr^{-} \leftrightharpoons HPCr^{2-} + H^{+}$	4.5	2.66
	$MgHPCr \leftrightharpoons HPCr^{2-} + Mg^{2+}$	1.6	8.19
	$KHPCr^{-} \leftrightharpoons HPCr^{2-} + K^{+}$	0.31	—
Cr	$H_2Cr^{+} \leftrightharpoons HCr + H^{+}$	2.3	—
Pi	$H_2Pi^{-} \leftrightharpoons HPi^{2-} + H^{+}$	6.75	3
	$MgHPi \leftrightharpoons HPi^{2-} + Mg^{2+}$	1.65	−12
	$MgH_2Pi^{+} \leftrightharpoons H_2Pi^{-} + Mg^{2+}$	1.19	—
	$KHPi^{-} \leftrightharpoons HPi^{2-} + K^{+}$	0.5	—

Table 2.3

Reactants, reference species, Gibbs free energy of formation, and binding constants for Eqs. (2.66) and (2.76) (298.15 K, 1 *M* reactants, I = 0.17 *M*, P = 1 atm)

Reactant	**Reference species**	$\Delta_f G^o$ **(kJ/mol)**	**Ion bound species**	pK^a
Water	H_2O	−235.74	—	—
Oxaloacete	OAA^{2-}	−794.41	$MgOAA^0$	0.8629[b]
Acetyl-co- enzyme A	$ACCOA^0$	−178.19	—	—
Citrate	CIT^{3-}	−1165.59	$HCIT^{2-}$	5.63
			$MgCIT^-$	3.37[b]
			$KCIT^{2-}$	0.339[b]
Coenzyme A	$COAS^-$	−0.72	$COASH^0$	8.13
Adenosine triphosphate (ATP)	ATP^{4-}	−2771.00	$HATP^{3-}$	6.59
			$MgATP^{2-}$	3.82
			$KATP^{3-}$	1.01
Adenosine diphosphate (ADP)	ADP^{3-}	−1903.96	$HADP^{2-}$	6.42
			$MgADP^-$	2.79
			$KADP^{2-}$	0.882
Inorganic phosphate (Pi)	HPO_4^{2-}	−1098.27	$H_2PO_4^-$	6.71
			$MgHPO_4^0$	1.69
			$KHPO_4^-$	−0.0074

[a] All values from Alberty (2003) unless otherwise noted.

[b] NIST Database 46: Critical Stability Constants.